



Measurement of the WZ production cross section in pp collisions at $\sqrt{s} = 7$ and 8 TeV and search for anomalous triple gauge couplings at $\sqrt{s} = 8$ TeV

CMS Collaboration*

CERN, 1211 Geneva 23, Switzerland

Received: 19 September 2016 / Accepted: 1 March 2017 / Published online: 12 April 2017
© CERN for the benefit of the CMS collaboration 2017. This article is an open access publication

Abstract The WZ production cross section is measured by the CMS experiment at the CERN LHC in proton–proton collision data samples corresponding to integrated luminosities of 4.9 fb^{-1} collected at $\sqrt{s} = 7 \text{ TeV}$, and 19.6 fb^{-1} at $\sqrt{s} = 8 \text{ TeV}$. The measurements are performed using the fully-leptonic WZ decay modes with electrons and muons in the final state. The measured cross sections for $71 < m_Z < 111 \text{ GeV}$ are $\sigma(\text{pp} \rightarrow \text{WZ}; \sqrt{s} = 7 \text{ TeV}) = 20.14 \pm 1.32 \text{ (stat)} \pm 0.38 \text{ (theo)} \pm 1.06 \text{ (exp)} \pm 0.44 \text{ (lumi)} \text{ pb}$ and $\sigma(\text{pp} \rightarrow \text{WZ}; \sqrt{s} = 8 \text{ TeV}) = 24.09 \pm 0.87 \text{ (stat)} \pm 0.80 \text{ (theo)} \pm 1.40 \text{ (exp)} \pm 0.63 \text{ (lumi)} \text{ pb}$. Differential cross sections with respect to the Z boson p_T , the leading jet p_T , and the number of jets are obtained using the $\sqrt{s} = 8 \text{ TeV}$ data. The results are consistent with standard model predictions and constraints on anomalous triple gauge coupling constants are obtained.

1 Introduction

The measurement of the production of electroweak heavy vector boson pairs (diboson production) in proton–proton collisions represents an important test of the standard model (SM) description of electroweak and strong interactions at the TeV scale. Diboson production is sensitive to the self-interactions between electroweak gauge bosons as predicted by the $SU(2)_L \times U(1)_Y$ gauge structure of electroweak interactions. Triple and quartic gauge couplings (TGCs and QGCs) can be affected by new physics phenomena involving new particles at higher energy scales. The WZ cross section measured in this paper is sensitive to WWZ couplings, which are non-zero in the SM. WZ production also represents an important background in several searches for physics beyond the SM, such as the search for the SM Higgs boson [1], searches for new resonances [2, 3], or supersymmetry [4–7].

We present a study of WZ production in proton–proton collisions based on data recorded by the CMS detector at the CERN LHC in 2011 and 2012, corresponding to integrated luminosities of 4.9 fb^{-1} collected at $\sqrt{s} = 7 \text{ TeV}$, and 19.6 fb^{-1} collected at $\sqrt{s} = 8 \text{ TeV}$. The measurements use purely leptonic final states in which the Z boson decays into a pair of electrons or muons, and the W boson decays into a neutrino and an electron or a muon. At leading order (LO) within the SM, WZ production in proton–proton collisions occurs through quark–antiquark interactions in the s -, t -, and u -channels, as illustrated by the Feynman diagrams shown in Fig. 1. Among them, only the s -channel includes a TGC vertex. Our measured final states also include contributions from diagrams where the Z boson is replaced with a virtual photon (γ^*) and thus include $W\gamma^*$ production. We refer to the final states as WZ production because the Z contribution is dominant for the phase space of this measurement. Hadron collider WZ production has been previously observed at both the Tevatron [8, 9] and the LHC [10–15].

We first describe measurements of the inclusive WZ production cross section at both centre-of-mass energies. The measurements are restricted to the phase space in which the invariant mass of the two leptons from the Z boson decay lies within 20 GeV of the nominal Z boson mass [16]. Using the larger integrated luminosity collected at $\sqrt{s} = 8 \text{ TeV}$, we also present measurements of the differential cross section as a function of the Z boson transverse momentum p_T , the number of jets produced in association with the WZ pair, and the p_T of the leading associated jet. The measurements involving jets are especially useful for probing the contribution of higher-order QCD processes to the cross section.

Finally, we present a search for anomalous WWZ couplings based on a measurement of the p_T spectrum of the Z boson. The search is formulated both in the framework of anomalous couplings and in an effective field theory approach.

* e-mail: cms-publication-committee-chair@cern.ch

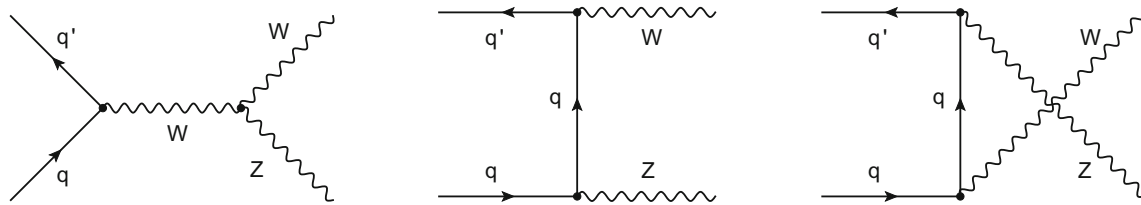


Fig. 1 Leading-order Feynman diagrams for WZ production in proton–proton collisions. The three diagrams represent contributions from (*left*) s -channel through TGC, (*middle*) t -channel, and (*right*) u -channel

2 The CMS detector

The central feature of the CMS apparatus is a superconducting solenoid of 6 m internal diameter, providing a magnetic field of 3.8 T. Within the solenoid volume are a silicon pixel and strip tracker, a lead tungstate crystal electromagnetic calorimeter (ECAL), and a brass and scintillator hadron calorimeter (HCAL), each composed of a barrel and two endcap sections. Muons are measured in gas-ionization detectors embedded in the steel flux-return yoke outside the solenoid with detection planes made using three technologies: drift tubes, cathode strip chambers, and resistive-plate chambers. Extensive forward calorimetry complements the coverage provided by the barrel and endcap detectors. The silicon tracker measures charged particles within the pseudorapidity range $|\eta| < 2.50$. The ECAL provides coverage in $|\eta| < 1.48$ in a barrel region and $1.48 < |\eta| < 3.00$ in two endcap regions. Muons are measured in the range $|\eta| < 2.40$.

A more detailed description of the CMS detector, together with a definition of the coordinate system used and the relevant kinematic variables, can be found in Ref. [17].

3 Simulated samples

Several Monte Carlo (MC) event generators are used to simulate signal and background processes. The $W(Z/\gamma^*)$ signal for $m_{Z/\gamma^*} > 12$ GeV is generated at LO with MADGRAPH 5.1 [18] with up to two additional partons at matrix element level. The $t\bar{t}$, tW , and $q\bar{q} \rightarrow ZZ$ processes are generated at next-to-leading order (NLO) with POWHEG 2.0 [19–21]. The $gg \rightarrow ZZ$ process is simulated at leading order (one loop) with GG2ZZ [22]. Other background processes are generated at LO with MADGRAPH and include $Z + \text{jets}$, $W\gamma^*$ (with $m_{\gamma^*} < 12$ GeV), $Z\gamma$ as well as processes with at least three bosons in the decay chain comprised of WZZ , ZZZ , WWZ , WWW , $t\bar{t}W$, $t\bar{t}Z$, $t\bar{t}WW$, $t\bar{t}\gamma$ and $WW\gamma$, collectively referred to as VVV. For the modeling of anomalous triple gauge couplings (aTGCs), the NLO MCFM 6.3 [23] Monte Carlo program is used to compute weights that are applied to the WZ signal sample generated with MADGRAPH. In all samples, the parton-level events are interfaced with PYTHIA 6.426 [24] to describe parton showering, hadronization, fragmentation,

and the underlying event with the $Z2^*$ tune [25]. For LO generators, the default set of parton distribution functions (PDFs) used is CTEQ6L1 [26], while NLO CT10 [27] is used with NLO generators. For all processes, the detector response is simulated with a detailed description of the CMS detector, based on the GEANT4 package [28]. The event reconstruction is performed with the same algorithms as are used for data. The simulated samples include additional interactions per bunch crossing (pileup). Simulated events are weighted so the pileup distribution in the simulation matches the one observed in data.

4 Event reconstruction and object identification

The measurement of the $WZ \rightarrow \ell\nu\ell'\nu'$ decay, where $\ell, \ell' = e$ or μ , relies on the effective identification of electrons and muons, and an accurate measurement of missing transverse momentum. The lepton selection requirements used in this measurement are the same as those used in the Higgs boson $H \rightarrow WW \rightarrow \ell\ell'\nu\nu$ measurement [1]. The kinematic properties of the final-state leptons in those two processes are very similar and the two measurements are affected by similar sources of lepton backgrounds.

Events are required to be accepted by one of the following double-lepton triggers: two electrons or two muons with transverse momentum thresholds of 17 GeV for the leading lepton, and 8 GeV for the trailing one. For the 8 TeV data sample, events are also accepted when an electron-muon pair satisfies the same momentum criteria.

A particle-flow (PF) algorithm [29,30] is used to reconstruct and identify each individual particle with an optimized combination of information from the various elements of the CMS detector: clusters of energy deposits measured by the calorimeters, and charged-particle tracks identified in the central tracking system and the muon detectors.

Electrons are reconstructed by combining information from the ECAL and tracker [31]. Their identification relies on a multivariate regression technique that combines observables sensitive to the amount of bremsstrahlung along the electron trajectory, the geometrical and momentum matching between the electron trajectory in the tracker and the energy deposit in the calorimeter, as well as the shower shape. Muons

are reconstructed using information from both the tracker and the muon spectrometer [32]. They must satisfy requirements on the number of hits in the layers of the tracker and in the muon spectrometer, and on the quality of the full track fit. All lepton candidates are required to be consistent with the primary vertex of the event, which is chosen as the vertex with the highest $\sum p_T^2$ of its associated tracks. This criterion provides the correct assignment for the primary vertex in more than 99% of both signal and background events for the pileup distribution observed in data. Both electrons and muons are required to have $p_T > 10 \text{ GeV}$. Electrons (muons) must satisfy $|\eta| < 2.5$ (2.4).

Charged leptons from W and Z boson decays are mostly isolated from other final-state particles in the event. Consequently, the selected leptons are required to be isolated from other activity in the event to reduce the backgrounds from hadrons that are misidentified as leptons or from leptons produced in hadron decays when they occur inside or near hadronic jets. The separation between two reconstructed objects in the detector is measured with the variable $\Delta R = \sqrt{(\Delta\eta)^2 + (\Delta\phi)^2}$, where ϕ is the azimuthal angle. To measure the lepton isolation, we consider a $\Delta R = 0.3$ cone around the lepton candidate track direction at the event vertex. An isolation variable is then built as the scalar p_T sum of all PF objects consistent with the chosen primary vertex, and contained within the cone. The contribution from the lepton candidate itself is excluded. For both electrons and muons a correction is applied to account for the energy contribution in the isolation cone due to pileup. In the case of electrons, the average energy density in the isolation cone due to pileup is determined event-by-event and is used to correct the isolation variable [33]. For muons, the pileup contribution from neutral particles to the isolation is estimated using charged particles associated with pileup interactions. This isolation variable is required to be smaller than about 10% of the candidate lepton p_T . The exact threshold value depends on the lepton flavour and detector region, and also on the data taking period: for 7 TeV data, it is 13% (9%) for electrons measured in the ECAL barrel (endcaps) and 12% for muons, while for 8 TeV data it is 15% for all electrons. For muons, a modified strategy has been used for 8 TeV data to account for the higher pileup conditions in order to reduce the dependence of this variable on the number of pileup interactions. It uses a multivariate algorithm based on the p_T sums of particles around the lepton candidates built for ΔR cones of different sizes [1].

The lepton reconstruction and selection efficiencies and associated uncertainties are determined using a tag-and-probe method with $Z \rightarrow \ell\ell$ events [34] chosen using the same criteria in data and simulation in several (p_T, η) bins. Ratios of efficiencies from data and simulation are calculated for each bin. To account for differences between data and simulation, the simulated samples are reweighted by these ratios

for each selected lepton in the event. The total uncertainty for the lepton efficiencies, including effects from trigger, reconstruction, and selection amounts to roughly 2% per lepton. The lepton selection criteria in the 7 and 8 TeV samples are chosen to maintain a stable efficiency throughout each data sample.

Jets are reconstructed from PF objects using the anti- k_T clustering algorithm [35, 36] with a size parameter R of 0.5. The energy of photons is obtained from the ECAL measurement. The energy of electrons is determined from a combination of the electron momentum at the primary interaction vertex as determined by the tracker, the energy of the corresponding ECAL cluster, and the energy sum of all bremsstrahlung photons spatially compatible with origination from the electron track. The energy of muons is obtained from the curvature of the corresponding track. The energy of charged hadrons is determined from a combination of their momentum measured in the tracker and the matching ECAL and HCAL energy deposits, corrected for the response function of the calorimeters to hadronic showers. Finally, the energy of neutral hadrons is obtained from the corresponding corrected ECAL and HCAL energy. The jet momentum is determined as the vector sum of all particle momenta in the jet. A correction is applied to jet energies to take into account the contribution from pileup. Jet energy corrections are derived from the simulation, and are confirmed with in situ measurements with the energy balance of dijet and photon + jet events [37]. The jet energy resolution amounts typically to 15% at 10 GeV, 8% at 100 GeV, and 4% at 1 TeV. Additional selection criteria are applied to each event to remove spurious jet-like features originating from isolated noise patterns in certain HCAL regions.

The missing transverse momentum vector \vec{p}_T^{miss} is defined as the negative vector sum of the transverse momenta of all reconstructed particles in an event. Its magnitude is referred to as E_T^{miss} .

5 Event selection and background estimates

We select $WZ \rightarrow \ell\nu\ell'\ell'$ decays with $W \rightarrow \ell\nu$ and $Z \rightarrow \ell'\ell'$, where ℓ and ℓ' are electrons or muons. These decays are characterized by a pair of same-flavour, opposite-charge, isolated leptons with an invariant mass consistent with a Z boson, together with a third isolated lepton and a significant amount of missing transverse energy E_T^{miss} associated with the escaping neutrino. We consider four different signatures corresponding to the flavour of the leptons in the final state: eee, ee μ , e $\mu\mu$ and $\mu\mu\mu$.

The four final states are treated independently for the cross section measurements and for the search for anomalous couplings, and are combined only at the level of the final results.

Unless explicitly stated otherwise, identical selection criteria are applied to the 7 and 8 TeV samples.

Candidate events are triggered by requiring the presence of two electrons or two muons. In the 8 TeV sample, events triggered by the presence of an electron and a muon are also accepted. The trigger efficiency for signal-like events that pass the event selection is measured to be larger than 99%. The candidate events are required to contain exactly three leptons matching all selection criteria. In the 8 TeV analysis, the invariant mass of the three leptons is required to be larger than 100 GeV. The Z boson candidates are built from two oppositely charged, same-flavour, isolated leptons. The leading lepton is required to have $p_T > 20$ GeV. The Z boson candidate invariant mass should lie within 20 GeV of the nominal Z boson mass: $71 < m_{\ell\ell} < 111$ GeV. If two matching pairs are found, the Z boson candidate with the mass closest to the nominal Z boson mass is selected. The remaining lepton is associated with the W boson and is required to have $p_T > 20$ GeV and to be separated from both leptons in the Z boson decay by $\Delta R > 0.1$. Finally, to account for the escaping neutrino, E_T^{miss} is required to be larger than 30 GeV.

Background sources with three reconstructed leptons include events with prompt leptons produced at the primary vertex or leptons from displaced vertices, as well as jets.

The background contribution from nonprompt leptons, dominated by $t\bar{t}$ and Z+jets events in which one of the three reconstructed leptons is misidentified, is estimated using a procedure similar to Ref. [38]. In this procedure, the amount of background in the signal region is estimated using the yields observed in several mutually exclusive samples containing events that did not satisfy some of the lepton selection requirements. The method uses the distinction between a loose and a tight lepton selection. The tight selection is identical to the one used in the final selection, while some of the lepton identification requirements used in the final selection are relaxed in the loose selection. The procedure starts from a sample, called the loose sample, with three leptons passing loose identification criteria and otherwise satisfying all other requirements of the WZ selection. This sample receives contributions from events with three prompt (p) leptons, two prompt leptons and one nonprompt (n) lepton, one prompt lepton and two nonprompt leptons, and three nonprompt leptons. The event yield of the loose sample N_{LLL} can thus be expressed as,

$$N_{\text{LLL}} = n_{\text{ppp}} + n_{\text{ppn}} + n_{\text{pnp}} + n_{\text{npp}} + n_{\text{nnp}} + n_{\text{npn}} + n_{\text{pnn}} + n_{\text{nnn}}. \quad (1)$$

In this expression, the first, second and third indices refer to the leading and subleading leptons from the Z boson decay and to the lepton from the W boson decay, respectively. The

loose sample can be divided into subsamples depending on whether each of the three leptons passes or fails the tight selection. The number of events in each subsample is labeled N_{ijk} with $i, j, k = \text{T}, \text{F}$ where T and F stand for leptons passing or failing the tight selection, respectively. The yield in each of these subsamples can be expressed as a linear combination of the unknown yields $n_{\alpha\beta\gamma}$ ($\alpha, \beta, \gamma \in \{\text{p}, \text{n}\}$),

$$N_{ijk} = \sum_{\alpha, \beta, \gamma \in \{\text{p}, \text{n}\}} C_{\alpha\beta\gamma}^{ijk} n_{\alpha\beta\gamma}, \quad i, j, k = \text{T}, \text{F}, \quad (2)$$

where the coefficients $C_{\alpha\beta\gamma}^{ijk}$ depend on the efficiencies ϵ_p and ϵ_n , which stand for the probabilities of prompt and non-prompt leptons, respectively, to pass the tight lepton selection provided they have passed the loose selection. For example, starting from Eq. (1), the number of events with all three leptons passing the tight selection N_{TTT} can be written as

$$\begin{aligned} N_{\text{TTT}} = & n_{\text{ppp}}\epsilon_{\text{p1}}\epsilon_{\text{p2}}\epsilon_{\text{p3}} + n_{\text{ppn}}\epsilon_{\text{p1}}\epsilon_{\text{p2}}\epsilon_{\text{n3}} + n_{\text{pnp}}\epsilon_{\text{p1}}\epsilon_{\text{n2}}\epsilon_{\text{p3}} \\ & + n_{\text{npp}}\epsilon_{\text{n1}}\epsilon_{\text{p2}}\epsilon_{\text{p3}} + n_{\text{nnp}}\epsilon_{\text{n1}}\epsilon_{\text{n2}}\epsilon_{\text{p3}} + n_{\text{nnp}}\epsilon_{\text{n1}}\epsilon_{\text{p2}}\epsilon_{\text{n3}} \\ & + n_{\text{pnn}}\epsilon_{\text{p1}}\epsilon_{\text{n2}}\epsilon_{\text{n3}} + n_{\text{nnn}}\epsilon_{\text{n1}}\epsilon_{\text{n2}}\epsilon_{\text{n3}}. \end{aligned} \quad (3)$$

The goal is to determine the number of events with three prompt leptons in the TTT sample, corresponding exactly to the selection used to perform the measurement. This yield is $n_{\text{ppp}}\epsilon_{\text{p1}}\epsilon_{\text{p2}}\epsilon_{\text{p3}}$. The number of events with three prompt leptons in the loose sample, n_{ppp} , is obtained by solving the set of linear Eq. (2).

Independent samples are used to measure the efficiencies ϵ_p and ϵ_n [38]. The prompt lepton efficiency ϵ_p is obtained from a $Z \rightarrow \ell\ell$ sample, while the nonprompt lepton efficiency ϵ_n is measured using a quantum chromodynamics (QCD) multijet sample. Events in this sample are triggered by a single lepton. The lepton selection used in these triggers is looser than the loose lepton selection referred to earlier in this section. The leading jet in the event is required to be well separated from the triggering lepton and have a transverse momentum larger than 50 GeV for the 7 TeV data sample, and larger than 35(20) GeV for the 8 TeV sample if the triggering lepton is an electron (muon). Events with leptons from Z decays are rejected by requiring exactly one lepton in the final state. To reject events with leptons from W decays, both the missing transverse energy and the W transverse mass are required to be less than 20 GeV. This selection provides a clean sample to estimate the nonprompt lepton efficiency. Both efficiencies ϵ_p and ϵ_n are measured in several lepton (p_T, η) bins. For 7 TeV (8 TeV) data, the measured nonprompt efficiencies for leptons are in the range 1–6% (1–10%), while they are in the range 1–5% (7–20%) for muons. The measured prompt efficiencies lie between 60 and 95% for electrons, and between 71 and 99% for muons for both the 7 and 8 TeV data samples.

Table 1 Expected and observed event yields at $\sqrt{s} = 7$ and 8 TeV. The contributions from $t\bar{t}$, $Z+jets$, and other processes with nonprompt leptons have been determined from data control samples, as described in the text. Backgrounds with at least three bosons in the decay chain com-

prised of WZZ , ZZZ , WWZ , WWW , $t\bar{t}W$, $t\bar{t}Z$, $t\bar{t}WW$, $t\bar{t}\gamma$ and $WW\gamma$ events, are referred to as VVV . Combined statistical and systematic uncertainties are shown, except for the WZ signal where only statistical uncertainties are shown

Sample	eee	$ee\mu$	$\mu\mu e$	$\mu\mu\mu$	Total
$\sqrt{s} = 7 \text{ TeV}; \mathcal{L} = 4.9 \text{ fb}^{-1}$					
Nonprompt leptons	2.2 ± 2.1	$1.5^{+4.8}_{-1.5}$	$2.4^{+5.1}_{-2.4}$	$1.8^{+7.5}_{-1.8}$	$7.9^{+13.0}_{-5.0}$
ZZ	2.0 ± 0.3	3.5 ± 0.5	2.7 ± 0.4	5.1 ± 0.7	13.3 ± 1.9
$Z\gamma$	0	0	0.5 ± 0.5	0	0.5 ± 0.5
VVV	1.6 ± 0.8	2.0 ± 1.0	2.4 ± 1.2	3.0 ± 1.5	9.0 ± 4.5
Total background (N_{bkg})	3.8 ± 2.3	$6.0 \pm ^{+4.9}_{-1.9}$	$8.0^{+5.1}_{-2.4}$	$9.9^{+7.7}_{-2.4}$	$30.7^{+13.9}_{-7.0}$
WZ	44.7 ± 0.5	49.8 ± 0.5	56.0 ± 0.5	73.8 ± 0.6	224.3 ± 1.1
Total expected	50.5 ± 2.3	$56.8^{+5.0}_{-1.9}$	$64.0^{+5.3}_{-2.8}$	$83.7^{+7.7}_{-2.5}$	$255^{+14.0}_{-7.0}$
Data (N_{obs})	64	62	70	97	293
$\sqrt{s} = 8 \text{ TeV}; \mathcal{L} = 19.6 \text{ fb}^{-1}$					
Nonprompt leptons	18.4 ± 12.7	32.0 ± 21.0	54.4 ± 33.0	62.4 ± 37.7	167.1 ± 55.8
ZZ	2.1 ± 0.3	2.4 ± 0.4	3.2 ± 0.5	4.7 ± 0.7	12.3 ± 1.0
$Z\gamma$	3.4 ± 1.3	0.4 ± 0.4	5.2 ± 1.8	0	9.1 ± 2.2
$W\gamma^*$	0	0	0	2.8 ± 1.0	2.8 ± 1.0
VVV	6.7 ± 2.2	8.7 ± 2.8	11.6 ± 3.8	14.8 ± 5.1	41.9 ± 7.3
Total background (N_{bkg})	30.6 ± 13.0	43.5 ± 21.2	74.4 ± 33.3	84.7 ± 38.1	233.2 ± 56.3
WZ	211.1 ± 1.6	262.1 ± 1.8	346.7 ± 2.1	447.8 ± 2.4	1267.7 ± 4.0
Total expected	241.6 ± 13.1	305.7 ± 21.3	421.0 ± 33.3	532.4 ± 38.2	1500.8 ± 56.5
Data (N_{obs})	258	298	435	568	1559

The number of events with nonprompt leptons in each final state obtained with this method is given in Table 1. While these results include the contribution of events with any number of misidentified leptons, simulation studies show that the contribution from backgrounds with two or three misidentified leptons, such as $W+jets$ or QCD multijet processes, is negligible, so the nonprompt lepton background is completely dominated by $t\bar{t}$ and $Z+jets$ processes.

The remaining background is composed of events with three prompt leptons, such as the $ZZ \rightarrow 2\ell 2\ell'$ process in which one of the four final-state leptons has not been identified, as well as processes with three or more heavy bosons in the final states (VVV), and the $W\gamma^*$ process, with $\gamma^* \rightarrow \ell^+ \ell^-$. These backgrounds are estimated from simulation. The relevant $W\gamma^*$ process is defined for low γ^* masses, $m_{\gamma^*} < 12 \text{ GeV}$, so it does not overlap with the $W\gamma^*$ process included in the signal simulation and it is simulated separately. It is considered a background since it does not fall in the fiducial phase space of the proposed measurement. Such $W\gamma^*$ processes would be accepted by the event selection only if the charged lepton from the W decay is wrongly interpreted as coming from the Z/γ^* decay. The contribution of $Z\gamma$ events in which the photon is misidentified as a

lepton is also determined from simulation. Prompt photons will not contribute to a nonprompt lepton signal since photons and electrons have a similar signature in the detector. Prompt photons in $Z\gamma$ events will also typically be isolated from other final state particles.

We finally consider the contribution of WZ decays, in which either the W or Z boson decays to a τ lepton. Such decays are considered a background to the signal. Their contribution is subtracted using the fraction of selected WZ decays that have τ leptons in the final state. This fraction, labeled f_τ , is estimated from simulation for each of the four final states, and lies in between 6.5 and 7.6%. This background is almost entirely composed of WZ events with $W \rightarrow \tau\nu$ decays where the τ lepton subsequently decays into an electron or a muon.

After applying all selection criteria, 293 (1559) events are selected from the 7(8) TeV data corresponding to an integrated luminosity of $4.9(19.6) \text{ fb}^{-1}$. The yields for each leptonic channel, together with the expectations from MC simulation and data control samples are given in Table 1. The inclusive distributions of the dilepton invariant mass $m_{\ell\ell}$ for both 7 and 8 TeV data samples are shown in Fig. 2.

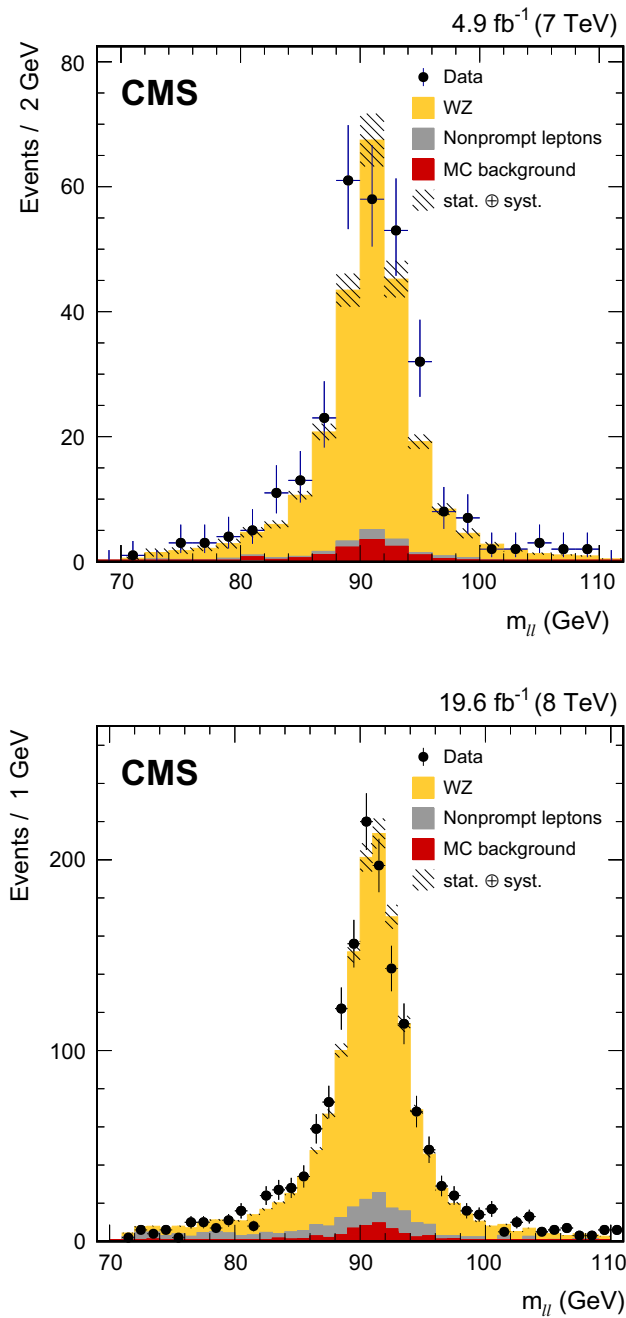


Fig. 2 Distributions of the dilepton invariant mass $m_{\ell\ell}$ in the WZ candidate events in 7 TeV (top) and 8 TeV (bottom) data. Points represent data and the shaded histograms represent the WZ signal and the background processes. The contribution from nonprompt leptons, dominated by the $t\bar{t}$ and Z+jets production, is obtained from data control samples. The contribution from all other backgrounds, labeled ‘MC background’, as well as the signal contribution are determined from simulation

6 Systematic uncertainties

Systematic uncertainties can be grouped into three categories: the determination of signal efficiency, the estimation of background yields, and the luminosity measurement.

The first group includes uncertainties affecting the signal efficiency, referred to as ϵ_{sig} , which accounts for both detector geometrical acceptance and reconstruction and selection efficiencies. It is determined from simulation. Uncertainties on ϵ_{sig} depend on theoretical uncertainties in the PDFs. The PDF uncertainty is evaluated following the prescription in Ref. [39] using the CTEQ66 [26] PDF set. The uncertainties from normalization (μ_R) and factorization (μ_F) scales are estimated by varying both scales independently in the range $(0.5\mu_0, 2\mu_0)$ around their nominal value $\mu_0 = 0.5(M_Z + M_W)$ with the constraint $0.5 \leq \mu_R/\mu_F \leq 2$. The signal efficiency ϵ_{sig} is also affected by experimental uncertainties in the muon momentum scale and in the electron energy scale, lepton reconstruction and identification efficiencies, E_T^{miss} calibration scale, and pileup contributions. The effect of the muon momentum scale is estimated by varying the momentum of each muon in the simulated signal sample within the momentum scale uncertainty, which is 0.2% [32]. The same is done for electrons by varying the energy of reconstructed electrons within the uncertainty of the energy scale measurement, which is p_T and η dependent and is typically below 1%. The signal efficiency ϵ_{sig} also depends on the uncertainties in the ratios of observed-to-simulated efficiencies of the lepton trigger, reconstruction, and identification requirements. These ratios are used in the determination of ϵ_{sig} to account for efficiency differences between data and simulation. They are varied within their uncertainties, which depend on the lepton p_T and η and are about 1%. The uncertainty from the E_T^{miss} calibration is determined by scaling up and down the energy of all objects used for the E_T^{miss} determination within their uncertainties. Finally, ϵ_{sig} is affected by the uncertainty in the pileup contribution. Simulated events are reweighted to match the distribution of pileup interactions, which is estimated using a procedure that extracts the pileup from the instantaneous bunch luminosity and the total inelastic pp cross section. The weights applied to simulated events are changed by varying this cross section by 5% uncertainty [40].

The second group comprises uncertainties in the background yield. The uncertainty in the background from nonprompt leptons [38] is estimated by varying the leading jet p_T threshold used to select the control sample of misidentified leptons, since the energy of the leading jet determines the composition of the sample. The uncertainties from other background processes, whose contributions are determined from simulation, are calculated by varying their predicted cross sections within uncertainties. The cross sections are varied by 15% (14%) for ZZ, by 15% (7%) for $Z\gamma$, by 50% (50%) for the VVV processes, and by 20% for $W\gamma^*$ for the 8 TeV (7 TeV) measurements, based on the uncertainties of the measurements of these processes [41–45].

Finally, the uncertainty in the measurement of the integrated luminosity is 2.2 (2.6)% for 7 (8) TeV data [46, 47].

Table 2 Summary of relative uncertainties, in units of percent, in the WZ cross section measurement at 7 and 8 TeV

Source	$\sqrt{s} = 7 \text{ TeV}$				$\sqrt{s} = 8 \text{ TeV}$			
	eee	ee μ	$\mu\mu e$	$\mu\mu\mu$	eee	ee μ	$\mu\mu e$	$\mu\mu\mu$
Renorm. and fact. scales	1.3	1.3	1.3	1.3	3.0	3.0	3.0	3.0
PDFs	1.4	1.4	1.4	1.4	1.4	1.4	1.4	1.4
Pileup	0.3	0.5	1.0	0.6	0.2	0.4	0.3	0.2
Lepton and trigger efficiency	2.9	2.7	2.0	1.4	3.4	2.5	2.5	3.2
Muon momentum scale	–	0.6	0.4	1.1	–	0.5	0.8	1.3
Electron energy scale	1.9	0.8	1.2	–	1.4	0.8	0.8	–
E_T^{miss}	3.7	3.4	4.3	3.7	1.5	1.5	1.6	1.2
ZZ cross section	0.5	0.9	0.6	0.9	0.1	0.1	0.1	0.1
Z γ cross section	0.0	0.0	0.1	0.0	0.2	0.0	0.2	0.0
t \bar{t} and Z+jets	2.7	6.5	6.3	6.0	4.6	7.2	6.1	7.7
Other simulated backgrounds	0.2	0.2	0.9	0.2	1.0	1.1	1.1	1.0
Total systematic uncertainty	6.1	7.8	8.1	7.2	7.0	8.6	7.7	9.2
Statistical uncertainty	13.5	13.9	13.1	11.0	7.7	7.2	6.4	5.2
Integrated luminosity uncertainty	2.2	2.2	2.2	2.2	2.6	2.6	2.6	2.6

A summary of all uncertainties is given in Table 2.

7 Results

7.1 Inclusive cross section measurement

The inclusive WZ cross section $\sigma(pp \rightarrow WZ + X)$ in the $\ell\nu\ell'\ell'$ final state is related to the number of observed events in that final state, N_{obs} , through the following expression,

$$\sigma(pp \rightarrow WZ + X) \mathcal{B}(W \rightarrow \ell\nu) \mathcal{B}(Z \rightarrow \ell'\ell') = (1 - f_\tau) \frac{N_{\text{obs}} - N_{\text{bkg}}}{\epsilon_{\text{sig}} \mathcal{L}},$$

where $\mathcal{B}(W \rightarrow \ell\nu)$ and $\mathcal{B}(Z \rightarrow \ell'\ell')$ are the W and Z boson leptonic branching fractions per lepton species, and f_τ accounts for the expected fraction of selected $WZ \rightarrow \ell\nu\ell'\ell'$ decays produced through at least one prompt τ decay in the final state after removing all other backgrounds. The number of expected background events is N_{bkg} , and the number of signal events is determined by subtracting N_{bkg} from the observed data N_{obs} . The signal efficiency ϵ_{sig} accounts for both detector geometrical acceptance and reconstruction and selection efficiencies. It is obtained for each of the four final states using the simulated WZ sample by calculating the ratio of the number of events passing the full selection to the number of generated $WZ \rightarrow \ell\nu\ell'\ell'$ events with $71 < m_{\ell\nu\ell'} < 111 \text{ GeV}$, where $m_{\ell\nu\ell'}$ is the dilepton mass of the two leptons from the Z boson decay prior to final state photon radiation. Only events decaying into the respective final state are considered in both the numerator and denominator of this fraction. The resulting cross section values are

reported in Table 3 for the four leptonic channels. There is good agreement among the four channels for both the 7 and 8 TeV data.

These four measurements are combined using the best linear unbiased estimator (BLUE) method [48]. We have assumed full correlation for all uncertainties common to different channels. Combining the four leptonic channels, the total WZ cross section for $71 < m_Z < 111 \text{ GeV}$, at 7 and 8 TeV, is measured to be

$$\begin{aligned} \sigma(pp \rightarrow WZ; \sqrt{s} = 7 \text{ TeV}) &= 20.14 \pm 1.32 \text{ (stat)} \pm 0.38 \text{ (theo)} \pm 1.06 \text{ (exp)} \\ &\pm 0.44 \text{ (lumi) pb.} \\ \sigma(pp \rightarrow WZ; \sqrt{s} = 8 \text{ TeV}) &= 24.09 \pm 0.87 \text{ (stat)} \pm 0.80 \text{ (theo)} \pm 1.40 \text{ (exp)} \\ &\pm 0.63 \text{ (lumi) pb.} \end{aligned}$$

These results can be compared with recent calculations at NLO and next-to-next-to-leading order (NNLO) in QCD via MATRIX [49]. The NLO (NNLO) predictions are $17.72^{+5.3\%}_{-1.8\%}$ ($19.18^{+1.7\%}_{-1.8\%}$) pb at 7 TeV, and $21.80^{+5.1\%}_{-3.9\%}$ ($23.68 \pm 1.8\%$) pb at 8 TeV, where uncertainties include only scale variations. All these predictions are in agreement with the measured values within uncertainties. The NLO predictions are slightly lower than the measured values, and a better agreement is observed for the NNLO observations at both centre-of-mass energies. The ratios of the inclusive cross sections for the individual and combined results to the NLO and NNLO predictions are shown in Fig. 3.

The total WZ production cross sections for different centre-of-mass energies from the CMS [13] and ATLAS [10–

Table 3 Measured WZ cross section in the four leptonic channels at $\sqrt{s} = 7$ and 8 TeV

Channel	$\sigma(pp \rightarrow WZ; \sqrt{s} = 7 \text{ TeV}) [\text{pb}]$
eee	$22.46 \pm 3.12 (\text{stat}) \pm 0.43 (\text{theo}) \pm 1.33 (\text{exp}) \pm 0.49 (\text{lumi})$
ee μ	$19.04 \pm 2.75 (\text{stat}) \pm 0.36 (\text{theo}) \pm 1.50 (\text{exp}) \pm 0.42 (\text{lumi})$
$\mu\mu e$	$19.13 \pm 2.60 (\text{stat}) \pm 0.37 (\text{theo}) \pm 1.56 (\text{exp}) \pm 0.42 (\text{lumi})$
$\mu\mu\mu$	$20.36 \pm 2.31 (\text{stat}) \pm 0.39 (\text{theo}) \pm 1.48 (\text{exp}) \pm 0.45 (\text{lumi})$
Channel	$\sigma(pp \rightarrow WZ; \sqrt{s} = 8 \text{ TeV}) [\text{pb}]$
eee	$24.80 \pm 1.92 (\text{stat}) \pm 0.82 (\text{theo}) \pm 1.53 (\text{exp}) \pm 0.64 (\text{lumi})$
ee μ	$22.38 \pm 1.62 (\text{stat}) \pm 0.74 (\text{theo}) \pm 1.78 (\text{exp}) \pm 0.58 (\text{lumi})$
$\mu\mu e$	$23.94 \pm 1.52 (\text{stat}) \pm 0.79 (\text{theo}) \pm 1.66 (\text{exp}) \pm 0.62 (\text{lumi})$
$\mu\mu\mu$	$24.93 \pm 1.29 (\text{stat}) \pm 0.83 (\text{theo}) \pm 2.14 (\text{exp}) \pm 0.65 (\text{lumi})$

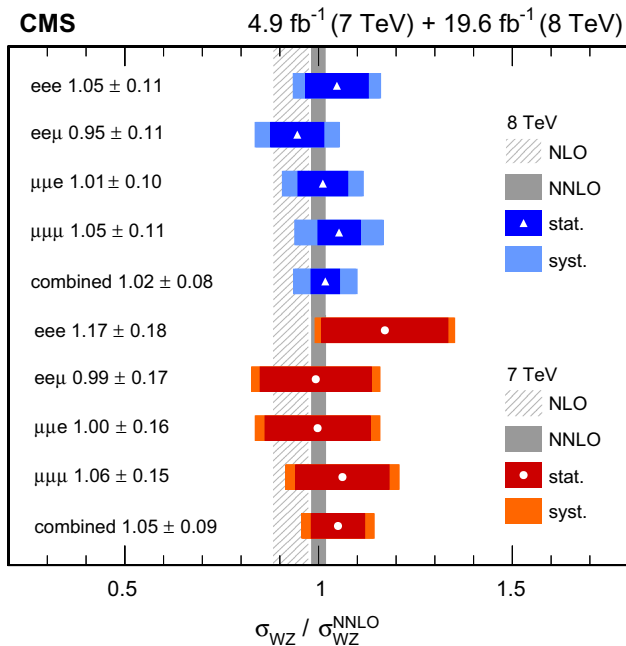


Fig. 3 Ratio of measured inclusive cross sections to NNLO predictions. The vertical gray bands represent the theoretical uncertainties at 7 and 8 TeV

[12] experiments are compared to theoretical predictions calculated with MCFM (NLO) and MATRIX (NNLO) in Fig. 4. The theoretical predictions describe, within the uncertainties, the energy dependence of the measured cross sections. The band around the theoretical predictions in this figure reflects uncertainties generated by varying the factorization and renormalization scales up and down by a factor of two and also the (PDF+ α_S) uncertainty of NNPDF3.0 for NLO predictions.

7.2 Differential cross section measurement

Using the larger available integrated luminosity in the 8 TeV sample, we measure the differential WZ cross sections as a

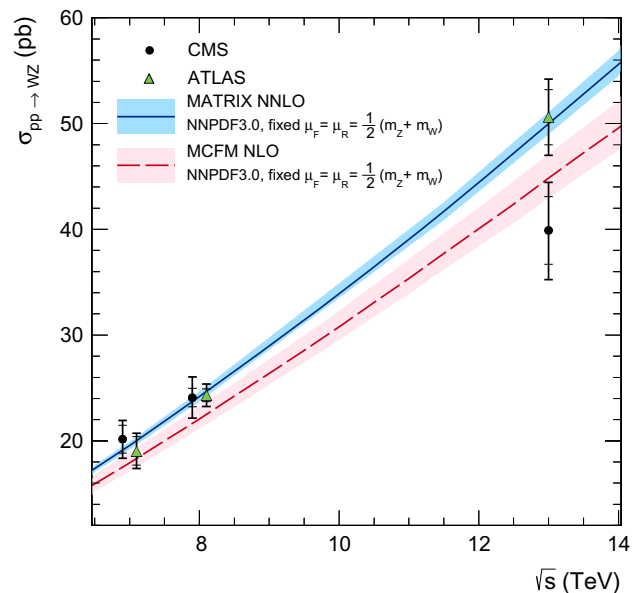


Fig. 4 The WZ total cross section as a function of the proton–proton centre-of-mass energy. Results from the CMS and ATLAS experiments are compared to the predictions of MCFM and MATRIX. The data uncertainties are statistical (inner bars) and statistical plus systematic added in quadrature (outer bars). The uncertainties covered by the band around the theoretical predictions are described in the text. The theoretical predictions and the CMS 13 TeV cross section are calculated for the Z boson mass window 60–120 GeV. The CMS 7 and 8 TeV cross sections presented in this paper are calculated for the Z boson mass window 71–111 GeV (estimated correction factor 2%), while all ATLAS measurements are performed with the Z boson mass window 66–116 GeV (1%)

function of three different observables: the Z boson p_T , the number of jets produced in association with the $\ell\nu\ell'\ell'$ final state, and the p_T of the leading accompanying jet. For the latter two measurements, the differential cross sections are defined for generated jets built from all stable particles using the anti- k_T algorithm [35] with a distance parameter of 0.5, but excluding the electrons, muons, and neutrinos from the W and Z boson decays. Jets are required to have $p_T > 30 \text{ GeV}$ and $|\eta| < 2.5$. They also must be separated from the charged leptons from the W and Z boson decays by $\Delta R(\text{jet}, \ell) > 0.5$.

Table 4 Differential WZ cross section as a function of the Z transverse momentum at $\sqrt{s} = 8$ TeV for the four leptonic final states. The first uncertainty is statistical, the second is systematic, and the third is the integrated luminosity

p_T^Z [GeV]	$d\sigma/dp_T^Z$ [pb /GeV]			
	eee	ee μ	$\mu\mu e$	$\mu\mu\mu$
0–20	(1.63 ± 0.90 ± 0.22 ± 0.04) $\times 10^{-1}$	(9.3 ± 6.8 ± 1.3 ± 0.2) $\times 10^{-2}$	(1.68 ± 0.92 ± 0.21 ± 0.04) $\times 10^{-1}$	(2.01 ± 1.00 ± 0.20 ± 0.05) $\times 10^{-1}$
	(3.9 ± 1.4 ± 0.5 ± 0.1) $\times 10^{-1}$	(3.17 ± 1.26 ± 0.39 ± 0.08) $\times 10^{-1}$	(2.76 ± 1.18 ± 0.62 ± 0.07) $\times 10^{-1}$	(3.42 ± 1.31 ± 0.57 ± 0.09) $\times 10^{-1}$
	(3.14 ± 1.25 ± 0.60 ± 0.08) $\times 10^{-1}$	(2.70 ± 1.16 ± 0.43 ± 0.07) $\times 10^{-1}$	(2.29 ± 1.07 ± 0.48 ± 0.06) $\times 10^{-1}$	(2.82 ± 1.19 ± 0.56 ± 0.07) $\times 10^{-1}$
	(1.69 ± 0.92 ± 0.30 ± 0.04) $\times 10^{-1}$	(2.07 ± 1.02 ± 0.31 ± 0.05) $\times 10^{-1}$	(2.31 ± 1.07 ± 0.33 ± 0.06) $\times 10^{-1}$	(2.03 ± 1.01 ± 0.31 ± 0.05) $\times 10^{-1}$
20–40	(1.27 ± 0.80 ± 0.23 ± 0.03) $\times 10^{-1}$	(1.02 ± 0.71 ± 0.17 ± 0.03) $\times 10^{-1}$	(1.30 ± 0.81 ± 0.25 ± 0.03) $\times 10^{-1}$	(1.25 ± 0.79 ± 0.21 ± 0.03) $\times 10^{-1}$
	(8.1 ± 6.4 ± 2.2 ± 0.2) $\times 10^{-2}$	(2.76 ± 3.72 ± 1.55 ± 0.07) $\times 10^{-2}$	(5.0 ± 5.0 ± 1.4 ± 0.1) $\times 10^{-2}$	(7.8 ± 6.3 ± 1.4 ± 0.2) $\times 10^{-2}$
	(5.8 ± 5.4 ± 0.9 ± 0.1) $\times 10^{-2}$	(6.2 ± 5.6 ± 0.8 ± 0.2) $\times 10^{-2}$	(3.12 ± 3.95 ± 1.13 ± 0.08) $\times 10^{-2}$	(4.1 ± 4.5 ± 1.2 ± 0.1) $\times 10^{-2}$
	(1.07 ± 1.34 ± 0.58 ± 0.03) $\times 10^{-2}$	(1.09 ± 1.35 ± 0.62 ± 0.03) $\times 10^{-2}$	(2.73 ± 2.13 ± 0.56 ± 0.07) $\times 10^{-2}$	(1.46 ± 1.56 ± 0.53 ± 0.04) $\times 10^{-2}$
40–60	(3.66 ± 6.05 ± 1.58 ± 0.10) $\times 10^{-3}$	(9.0 ± 9.5 ± 1.7 ± 0.2) $\times 10^{-3}$	(7.4 ± 8.6 ± 1.7 ± 0.2) $\times 10^{-3}$	(5.8 ± 7.6 ± 1.8 ± 0.2) $\times 10^{-3}$
	(1.27 ± 0.80 ± 0.23 ± 0.03) $\times 10^{-1}$	(1.02 ± 0.71 ± 0.17 ± 0.03) $\times 10^{-1}$	(1.30 ± 0.81 ± 0.25 ± 0.03) $\times 10^{-1}$	(1.25 ± 0.79 ± 0.21 ± 0.03) $\times 10^{-1}$
	(8.1 ± 6.4 ± 2.2 ± 0.2) $\times 10^{-2}$	(2.76 ± 3.72 ± 1.55 ± 0.07) $\times 10^{-2}$	(5.0 ± 5.0 ± 1.4 ± 0.1) $\times 10^{-2}$	(7.8 ± 6.3 ± 1.4 ± 0.2) $\times 10^{-2}$
	(5.8 ± 5.4 ± 0.9 ± 0.1) $\times 10^{-2}$	(6.2 ± 5.6 ± 0.8 ± 0.2) $\times 10^{-2}$	(3.12 ± 3.95 ± 1.13 ± 0.08) $\times 10^{-2}$	(4.1 ± 4.5 ± 1.2 ± 0.1) $\times 10^{-2}$
60–80	(1.07 ± 1.34 ± 0.58 ± 0.03) $\times 10^{-2}$	(1.09 ± 1.35 ± 0.62 ± 0.03) $\times 10^{-2}$	(2.73 ± 2.13 ± 0.56 ± 0.07) $\times 10^{-2}$	(1.46 ± 1.56 ± 0.53 ± 0.04) $\times 10^{-2}$
	(3.66 ± 6.05 ± 1.58 ± 0.10) $\times 10^{-3}$	(9.0 ± 9.5 ± 1.7 ± 0.2) $\times 10^{-3}$	(7.4 ± 8.6 ± 1.7 ± 0.2) $\times 10^{-3}$	(5.8 ± 7.6 ± 1.8 ± 0.2) $\times 10^{-3}$
	(1.27 ± 0.80 ± 0.23 ± 0.03) $\times 10^{-1}$	(1.02 ± 0.71 ± 0.17 ± 0.03) $\times 10^{-1}$	(1.30 ± 0.81 ± 0.25 ± 0.03) $\times 10^{-1}$	(1.25 ± 0.79 ± 0.21 ± 0.03) $\times 10^{-1}$
	(8.1 ± 6.4 ± 2.2 ± 0.2) $\times 10^{-2}$	(2.76 ± 3.72 ± 1.55 ± 0.07) $\times 10^{-2}$	(5.0 ± 5.0 ± 1.4 ± 0.1) $\times 10^{-2}$	(7.8 ± 6.3 ± 1.4 ± 0.2) $\times 10^{-2}$
80–100	(1.07 ± 1.34 ± 0.58 ± 0.03) $\times 10^{-2}$	(1.09 ± 1.35 ± 0.62 ± 0.03) $\times 10^{-2}$	(2.73 ± 2.13 ± 0.56 ± 0.07) $\times 10^{-2}$	(1.46 ± 1.56 ± 0.53 ± 0.04) $\times 10^{-2}$
	(3.66 ± 6.05 ± 1.58 ± 0.10) $\times 10^{-3}$	(9.0 ± 9.5 ± 1.7 ± 0.2) $\times 10^{-3}$	(7.4 ± 8.6 ± 1.7 ± 0.2) $\times 10^{-3}$	(5.8 ± 7.6 ± 1.8 ± 0.2) $\times 10^{-3}$
	(1.27 ± 0.80 ± 0.23 ± 0.03) $\times 10^{-1}$	(1.02 ± 0.71 ± 0.17 ± 0.03) $\times 10^{-1}$	(1.30 ± 0.81 ± 0.25 ± 0.03) $\times 10^{-1}$	(1.25 ± 0.79 ± 0.21 ± 0.03) $\times 10^{-1}$
	(8.1 ± 6.4 ± 2.2 ± 0.2) $\times 10^{-2}$	(2.76 ± 3.72 ± 1.55 ± 0.07) $\times 10^{-2}$	(5.0 ± 5.0 ± 1.4 ± 0.1) $\times 10^{-2}$	(7.8 ± 6.3 ± 1.4 ± 0.2) $\times 10^{-2}$
100–120	(1.07 ± 1.34 ± 0.58 ± 0.03) $\times 10^{-2}$	(1.09 ± 1.35 ± 0.62 ± 0.03) $\times 10^{-2}$	(2.73 ± 2.13 ± 0.56 ± 0.07) $\times 10^{-2}$	(1.46 ± 1.56 ± 0.53 ± 0.04) $\times 10^{-2}$
	(3.66 ± 6.05 ± 1.58 ± 0.10) $\times 10^{-3}$	(9.0 ± 9.5 ± 1.7 ± 0.2) $\times 10^{-3}$	(7.4 ± 8.6 ± 1.7 ± 0.2) $\times 10^{-3}$	(5.8 ± 7.6 ± 1.8 ± 0.2) $\times 10^{-3}$
	(1.27 ± 0.80 ± 0.23 ± 0.03) $\times 10^{-1}$	(1.02 ± 0.71 ± 0.17 ± 0.03) $\times 10^{-1}$	(1.30 ± 0.81 ± 0.25 ± 0.03) $\times 10^{-1}$	(1.25 ± 0.79 ± 0.21 ± 0.03) $\times 10^{-1}$
	(8.1 ± 6.4 ± 2.2 ± 0.2) $\times 10^{-2}$	(2.76 ± 3.72 ± 1.55 ± 0.07) $\times 10^{-2}$	(5.0 ± 5.0 ± 1.4 ± 0.1) $\times 10^{-2}$	(7.8 ± 6.3 ± 1.4 ± 0.2) $\times 10^{-2}$
120–140	(1.07 ± 1.34 ± 0.58 ± 0.03) $\times 10^{-2}$	(1.09 ± 1.35 ± 0.62 ± 0.03) $\times 10^{-2}$	(2.73 ± 2.13 ± 0.56 ± 0.07) $\times 10^{-2}$	(1.46 ± 1.56 ± 0.53 ± 0.04) $\times 10^{-2}$
	(3.66 ± 6.05 ± 1.58 ± 0.10) $\times 10^{-3}$	(9.0 ± 9.5 ± 1.7 ± 0.2) $\times 10^{-3}$	(7.4 ± 8.6 ± 1.7 ± 0.2) $\times 10^{-3}$	(5.8 ± 7.6 ± 1.8 ± 0.2) $\times 10^{-3}$
	(1.27 ± 0.80 ± 0.23 ± 0.03) $\times 10^{-1}$	(1.02 ± 0.71 ± 0.17 ± 0.03) $\times 10^{-1}$	(1.30 ± 0.81 ± 0.25 ± 0.03) $\times 10^{-1}$	(1.25 ± 0.79 ± 0.21 ± 0.03) $\times 10^{-1}$
	(8.1 ± 6.4 ± 2.2 ± 0.2) $\times 10^{-2}$	(2.76 ± 3.72 ± 1.55 ± 0.07) $\times 10^{-2}$	(5.0 ± 5.0 ± 1.4 ± 0.1) $\times 10^{-2}$	(7.8 ± 6.3 ± 1.4 ± 0.2) $\times 10^{-2}$
140–200	(1.07 ± 1.34 ± 0.58 ± 0.03) $\times 10^{-2}$	(1.09 ± 1.35 ± 0.62 ± 0.03) $\times 10^{-2}$	(2.73 ± 2.13 ± 0.56 ± 0.07) $\times 10^{-2}$	(1.46 ± 1.56 ± 0.53 ± 0.04) $\times 10^{-2}$
	(3.66 ± 6.05 ± 1.58 ± 0.10) $\times 10^{-3}$	(9.0 ± 9.5 ± 1.7 ± 0.2) $\times 10^{-3}$	(7.4 ± 8.6 ± 1.7 ± 0.2) $\times 10^{-3}$	(5.8 ± 7.6 ± 1.8 ± 0.2) $\times 10^{-3}$
	(1.27 ± 0.80 ± 0.23 ± 0.03) $\times 10^{-1}$	(1.02 ± 0.71 ± 0.17 ± 0.03) $\times 10^{-1}$	(1.30 ± 0.81 ± 0.25 ± 0.03) $\times 10^{-1}$	(1.25 ± 0.79 ± 0.21 ± 0.03) $\times 10^{-1}$
	(8.1 ± 6.4 ± 2.2 ± 0.2) $\times 10^{-2}$	(2.76 ± 3.72 ± 1.55 ± 0.07) $\times 10^{-2}$	(5.0 ± 5.0 ± 1.4 ± 0.1) $\times 10^{-2}$	(7.8 ± 6.3 ± 1.4 ± 0.2) $\times 10^{-2}$
200–300	(1.07 ± 1.34 ± 0.58 ± 0.03) $\times 10^{-2}$	(1.09 ± 1.35 ± 0.62 ± 0.03) $\times 10^{-2}$	(2.73 ± 2.13 ± 0.56 ± 0.07) $\times 10^{-2}$	(1.46 ± 1.56 ± 0.53 ± 0.04) $\times 10^{-2}$
	(3.66 ± 6.05 ± 1.58 ± 0.10) $\times 10^{-3}$	(9.0 ± 9.5 ± 1.7 ± 0.2) $\times 10^{-3}$	(7.4 ± 8.6 ± 1.7 ± 0.2) $\times 10^{-3}$	(5.8 ± 7.6 ± 1.8 ± 0.2) $\times 10^{-3}$
	(1.27 ± 0.80 ± 0.23 ± 0.03) $\times 10^{-1}$	(1.02 ± 0.71 ± 0.17 ± 0.03) $\times 10^{-1}$	(1.30 ± 0.81 ± 0.25 ± 0.03) $\times 10^{-1}$	(1.25 ± 0.79 ± 0.21 ± 0.03) $\times 10^{-1}$
	(8.1 ± 6.4 ± 2.2 ± 0.2) $\times 10^{-2}$	(2.76 ± 3.72 ± 1.55 ± 0.07) $\times 10^{-2}$	(5.0 ± 5.0 ± 1.4 ± 0.1) $\times 10^{-2}$	(7.8 ± 6.3 ± 1.4 ± 0.2) $\times 10^{-2}$

The jets reconstructed from PF candidates, clustered by the same algorithm, have to fulfill the same requirements.

To obtain the cross section in each bin, the background contribution is first subtracted from the observed yield in each bin, in the same way as it was done for the inclusive cross section. The measured signal spectra are then corrected for the detector effects. These include efficiencies as well as bin-to-bin migrations due to finite resolution. Both effects are treated using the iterative D'Agostini unfolding technique [50], as implemented in ROOUNFOLD [51], with 5 iterations. The technique uses response matrices that relate the true distribution of an observable to the observed distribution after including detector effects. The response matrices are obtained using the signal MC sample for all four leptonic final states separately. The unfolded spectra are then used to obtain differential cross sections for all four leptonic final states. The four channels are combined bin-by-bin.

A few additional sources of systematic uncertainties need to be considered with respect to those described in Sect. 6. The measurements involving jets are affected by the experimental uncertainties in the jet energy scale and resolution. The effects on the response matrices are studied by smearing and scaling the jet energies within their uncertainties. Furthermore, an uncertainty due to the limited size of the simulated sample used to build the response matrices is also included. The unfolding procedure introduces statistical correlations between bins, which range from a few percent up to 40% in a few cases. These correlations are taken into account together with correlated systematic uncertainties by using a generalization of the BLUE method as described in Ref. [52]. The three measured differential cross sections are given in Tables 4, 5, and 6 for each of the four final states, and the combined results are given in Table 7. The combined differential cross sections are shown in Figs. 5 and 6.

Table 5 Differential WZ cross section as a function of the jet multiplicity at $\sqrt{s} = 8$ TeV for the four leptonic final states. Notations are as in Table 4

N_{jets}	$d\sigma/dN_{\text{jets}} [\text{pb}]$			
	eee	ee μ	$\mu\mu e$	$\mu\mu\mu$
0 Jets	16.60 \pm 4.07 \pm 1.04 \pm 0.43	15.68 \pm 3.96 \pm 1.03 \pm 0.41	14.97 \pm 3.87 \pm 0.93 \pm 0.39	18.78 \pm 4.33 \pm 1.11 \pm 0.49
	6.06 \pm 2.46 \pm 0.48 \pm 0.16	4.80 \pm 2.19 \pm 0.57 \pm 0.12	5.32 \pm 2.31 \pm 0.61 \pm 0.14	4.84 \pm 2.20 \pm 0.72 \pm 0.13
	2.43 \pm 1.56 \pm 0.34 \pm 0.06	1.75 \pm 1.32 \pm 0.32 \pm 0.05	2.93 \pm 1.71 \pm 0.26 \pm 0.08	1.54 \pm 1.24 \pm 0.32 \pm 0.04
3 Jets	(7.8 \pm 27.9 \pm 7.3 \pm 0.2) $\times 10^{-2}$	0.45 \pm 0.67 \pm 0.17 \pm 0.01	0.42 \pm 0.65 \pm 0.21 \pm 0.01	0.79 \pm 0.89 \pm 0.26 \pm 0.02

Table 6 Differential WZ cross section as a function of the leading jet transverse momentum at $\sqrt{s} = 8$ TeV for the four leptonic final states. Notations are as in Table 4

$p_T^{\text{leading jet}} [\text{GeV}]$	$d\sigma/dp_T^{\text{leading jet}} [\text{pb}/\text{GeV}]$			
	eee	ee μ	$\mu\mu e$	$\mu\mu\mu$
30–60	(1.22 \pm 0.64 \pm 0.34 \pm 0.03) $\times 10^{-1}$	(1.11 \pm 0.61 \pm 0.20 \pm 0.03) $\times 10^{-1}$	(1.10 \pm 0.61 \pm 0.24 \pm 0.03) $\times 10^{-1}$	(1.02 \pm 0.58 \pm 0.24 \pm 0.03) $\times 10^{-1}$
	(5.4 \pm 3.7 \pm 1.7 \pm 0.1) $\times 10^{-2}$	(4.3 \pm 3.3 \pm 2.1 \pm 0.1) $\times 10^{-2}$	(6.5 \pm 4.0 \pm 2.0 \pm 0.2) $\times 10^{-2}$	(6.3 \pm 4.0 \pm 2.3 \pm 0.2) $\times 10^{-2}$
	(2.96 \pm 2.43 \pm 1.57 \pm 0.08) $\times 10^{-2}$	(3.26 \pm 2.55 \pm 1.40 \pm 0.08) $\times 10^{-2}$	(3.9 \pm 2.8 \pm 1.2 \pm 0.1) $\times 10^{-2}$	(2.44 \pm 2.21 \pm 1.32 \pm 0.06) $\times 10^{-2}$
150–250	(1.18 \pm 1.09 \pm 0.29 \pm 0.03) $\times 10^{-2}$	(8.1 \pm 9.0 \pm 3.4 \pm 0.2) $\times 10^{-3}$	(1.07 \pm 1.03 \pm 0.61 \pm 0.03) $\times 10^{-2}$	(1.00 \pm 1.00 \pm 0.42 \pm 0.03) $\times 10^{-2}$

The differential cross sections are compared with the MCFM and MADGRAPH predictions. The MADGRAPH spectra are normalized to the NLO cross section as predicted by MCFM.

7.3 Anomalous triple gauge couplings limits

Triple gauge boson couplings are a consequence of the non-Abelian nature of the SM electroweak sector. Several extensions of the SM predict additional processes with multiple bosons in the final state so any observed deviation of diboson production cross sections from their SM predictions could be an early sign of new physics. The most general Lorentz invariant effective Lagrangian that describes WWV couplings, where $V = \gamma$ or Z , has 14 independent parameters [53,54], seven for $V = \gamma$ and seven for $V = Z$. Assuming charge conjugation (C) and parity (P) conservation, only six independent

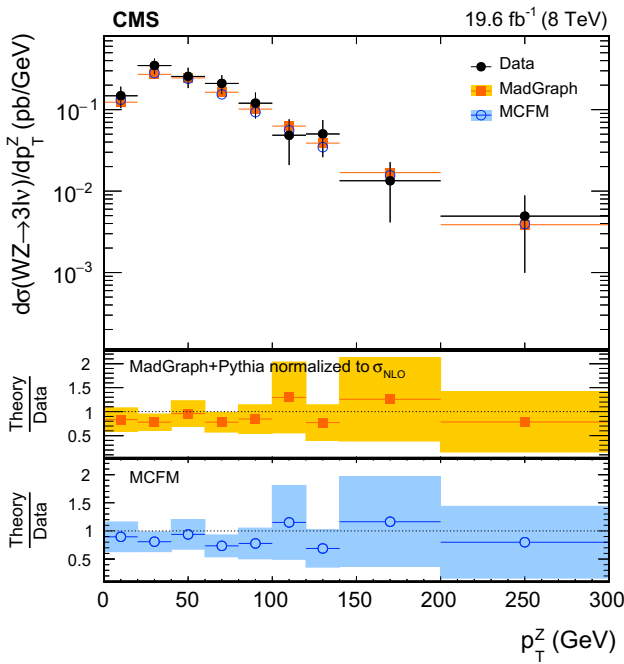
parameters remain. The effective Lagrangian, normalized by the electroweak coupling, is given by:

$$\begin{aligned} \frac{\mathcal{L}_{\text{TGC}}}{g_{WWV}} &= ig_1^V (W_{\mu\nu}^- W^{+\mu} V^\nu - W_\mu^- V_\nu W^{+\mu\nu}) \\ &+ i\kappa_V W_\mu^- W_\nu^+ V^{\mu\nu} + \frac{i\lambda_V}{M_W^2} W_{\delta\mu}^- W_\nu^{+\mu} V^{\nu\delta}, \end{aligned} \quad (4)$$

where $W^\pm_{\mu\nu} = \partial_\mu W^\pm_\nu - \partial_\nu W^\pm_\mu$, $V_{\mu\nu} = \partial_\mu V_\nu - \partial_\nu V_\mu$, and couplings $g_{WW\gamma} = -e$ and $g_{WWZ} = -e \cot \theta_W$, with θ_W being the weak mixing angle. Assuming electromagnetic gauge invariance, i.e. $g_1^\gamma = 1$, the remaining parameters that describe the WWV coupling are $g_1^Z, \kappa_Z, \kappa_\gamma, \lambda_Z$ and λ_γ . In the SM $\lambda_Z = \lambda_\gamma = 0$ and $g_1^Z = \kappa_Z = \kappa_\gamma = 1$. The couplings are further reduced to three independent parameters if one requires the Lagrangian to be $SU(2)_L \times U(1)_Y$ invariant (“LEP parameterization”) [55–57]:

Table 7 Combined result for the differential WZ cross sections at $\sqrt{s} = 8$ TeV

p_T^Z [GeV]	$d\sigma/dp_T^Z$ [pb/GeV]
0–20	$[1.48 \pm 0.40 \text{ (stat)} \pm 0.17 \text{ (syst)} \pm 0.04 \text{ (lumi)}] \times 10^{-1}$
20–40	$[3.47 \pm 0.60 \text{ (stat)} \pm 0.50 \text{ (syst)} \pm 0.09 \text{ (lumi)}] \times 10^{-1}$
40–60	$[2.56 \pm 0.54 \text{ (stat)} \pm 0.49 \text{ (syst)} \pm 0.07 \text{ (lumi)}] \times 10^{-1}$
60–80	$[2.10 \pm 0.47 \text{ (stat)} \pm 0.30 \text{ (syst)} \pm 0.05 \text{ (lumi)}] \times 10^{-1}$
80–100	$[1.20 \pm 0.37 \text{ (stat)} \pm 0.21 \text{ (syst)} \pm 0.03 \text{ (lumi)}] \times 10^{-1}$
100–120	$[4.9 \pm 2.3 \text{ (stat)} \pm 1.5 \text{ (syst)} \pm 0.1 \text{ (lumi)}] \times 10^{-2}$
120–140	$[5.0 \pm 2.2 \text{ (stat)} \pm 1.0 \text{ (syst)} \pm 0.1 \text{ (lumi)}] \times 10^{-2}$
140–200	$[1.34 \pm 0.73 \text{ (stat)} \pm 0.57 \text{ (syst)} \pm 0.03 \text{ (lumi)}] \times 10^{-2}$
200–300	$[4.9 \pm 3.6 \text{ (stat)} \pm 1.6 \text{ (syst)} \pm 0.1 \text{ (lumi)}] \times 10^{-3}$
N_{jets}	$d\sigma/dN_{\text{jets}}$ [pb]
0 Jets	$16.15 \pm 1.95 \text{ (stat)} \pm 0.88 \text{ (syst)} \pm 0.42 \text{ (lumi)}$
1 Jet	$5.27 \pm 1.11 \text{ (stat)} \pm 0.52 \text{ (syst)} \pm 0.14 \text{ (lumi)}$
2 Jets	$2.11 \pm 0.69 \text{ (stat)} \pm 0.27 \text{ (syst)} \pm 0.05 \text{ (lumi)}$
3 Jets	$0.196 \pm 0.227 \text{ (stat)} \pm 0.102 \text{ (syst)} \pm 0.005 \text{ (lumi)}$
$p_T^{\text{leading jet}}$ [GeV]	$d\sigma/dp_T^{\text{leading jet}}$ [pb/GeV]
30–60	$[1.12 \pm 0.30 \text{ (stat)} \pm 0.23 \text{ (syst)} \pm 0.03 \text{ (lumi)}] \times 10^{-1}$
60–100	$[5.5 \pm 1.8 \text{ (stat)} \pm 1.9 \text{ (syst)} \pm 0.1 \text{ (lumi)}] \times 10^{-2}$
100–150	$[3.06 \pm 1.20 \text{ (stat)} \pm 1.37 \text{ (syst)} \pm 0.08 \text{ (lumi)}] \times 10^{-2}$
150–250	$[1.04 \pm 0.48 \text{ (stat)} \pm 0.41 \text{ (syst)} \pm 0.03 \text{ (lumi)}] \times 10^{-2}$

**Fig. 5** Differential WZ cross section at $\sqrt{s} = 8$ TeV as a function of the Z boson transverse momentum. The measurement is compared with MCFM and MADGRAPH predictions. The MADGRAPH prediction is rescaled to the total NLO cross section as predicted by MCFM. The error bands in the ratio plots indicate the relative errors on the data in each bin and contain both statistical and systematic uncertainties

$$\Delta\kappa_Z = \Delta g_1^Z - \Delta\kappa_\gamma \tan^2 \theta_W, \quad \lambda = \lambda_\gamma = \lambda_Z, \quad (5)$$

where $\Delta\kappa_Z = \kappa_Z - 1$, $\Delta g_1^Z = g_1^Z - 1$ and $\Delta\kappa_\gamma = \kappa_\gamma - 1$.

In this analysis we measure $\Delta\kappa_Z$, λ , and Δg_1^Z from WZ production at 8 TeV. No form factor scaling is used for aTGCs, as this allows us to provide results without the bias that can be caused by the choice of the form factor energy dependence.

Another approach to the parametrization of anomalous couplings is through effective field theory (EFT), with the higher-order operators added to the SM Lagrangian as follows:

$$\mathcal{L}_{\text{EFT}} = \mathcal{L}_{\text{SM}} + \sum_{n=1}^{\infty} \sum_i \frac{c_i^{(n)}}{\Lambda^n} O_i^{(n+4)}. \quad (6)$$

Here O_i are the higher-order operators, the coefficients c_i are dimensionless, and Λ is the mass scale of new physics. Operators are suppressed if the accessible energy is low compared to the mass scale. There are three CP-even operators that contribute to WWZ TGC, O_{www} , O_W , and O_B . For the case of ‘LEP parametrization’ and no form factor scaling of aTGCs, the relations between parameters in the aTGCs and EFT approaches are as follows:

$$g_1^Z = 1 + c_W \frac{m_Z^2}{2\Lambda^2},$$

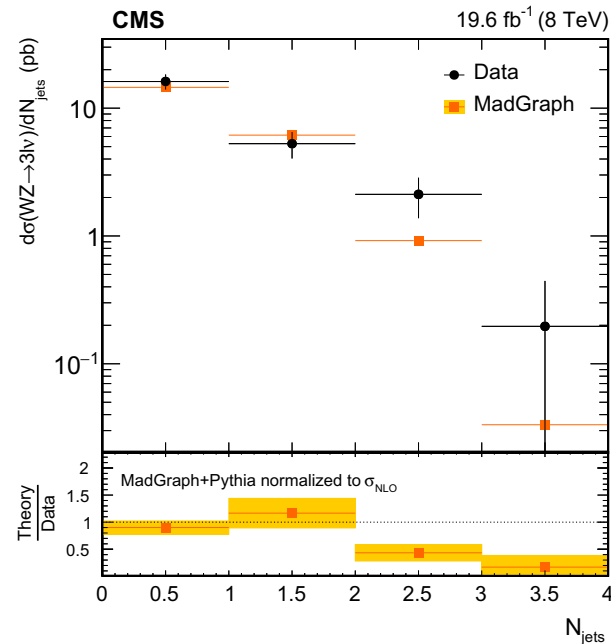
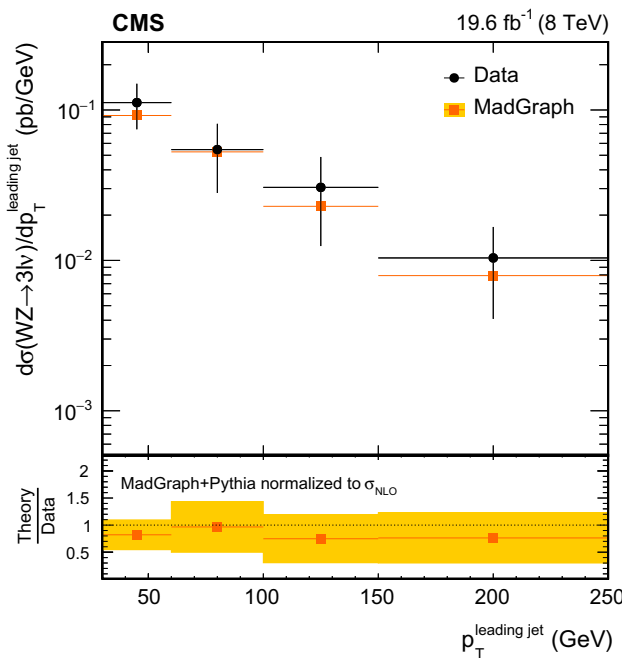


Fig. 6 Differential WZ cross section at $\sqrt{s} = 8$ TeV as a function of: (top) the leading jet transverse momentum; (bottom) the number of accompanying jets. The measurements are compared with MADGRAPH predictions. The MADGRAPH prediction is rescaled to the total NLO cross section as predicted by MCFM. The error bands in the ratio plots indicate the relative errors on the data in each bin and contain both statistical and systematic uncertainties

$$\kappa_\gamma = 1 + (c_W + c_B) \frac{m_W^2}{2\Lambda^2},$$

$$\kappa_Z = 1 + (c_W - c_B \tan^2 \theta_W) \frac{m_W^2}{2\Lambda^2},$$

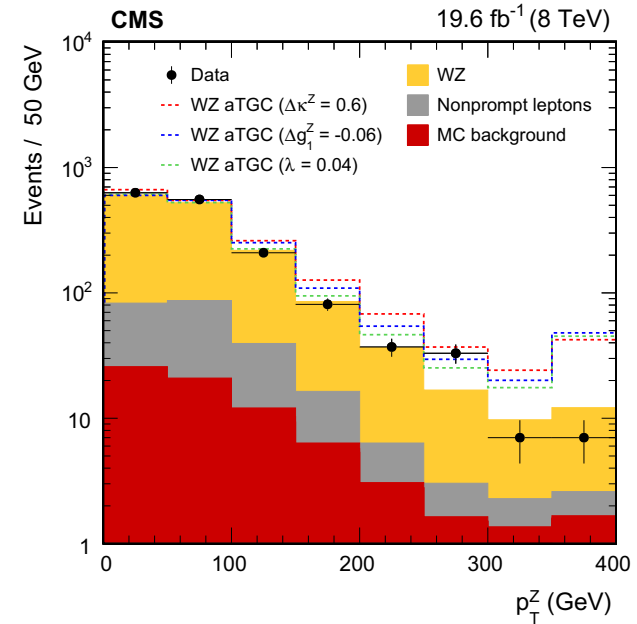
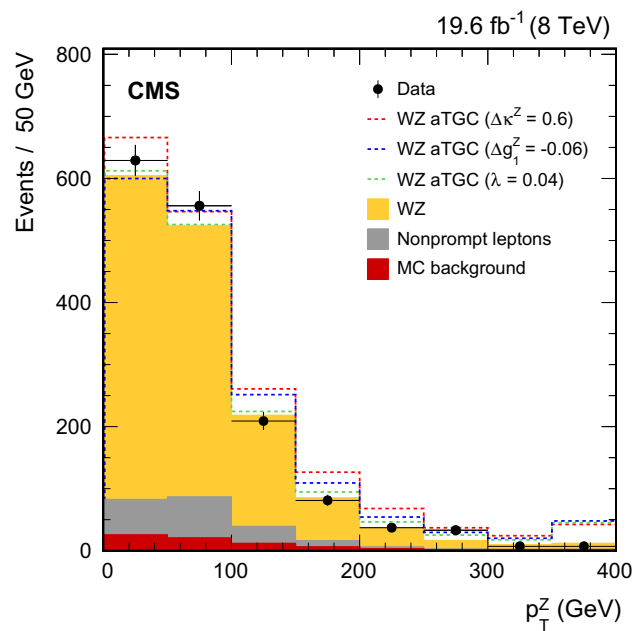


Fig. 7 Transverse momentum distribution of the Z boson candidates, in linear scale (top) and log scale (bottom) for all channels combined. The SM WZ contribution (light orange) is normalized to the predicted cross section from MCFM. Dashed lines correspond to aTGC expectations with different parameter values. The last bin includes the integral of the tail

$$\lambda_Z = \lambda_\gamma = c_{WWW} \frac{3g^2 m_W^2}{2\Lambda^2}.$$

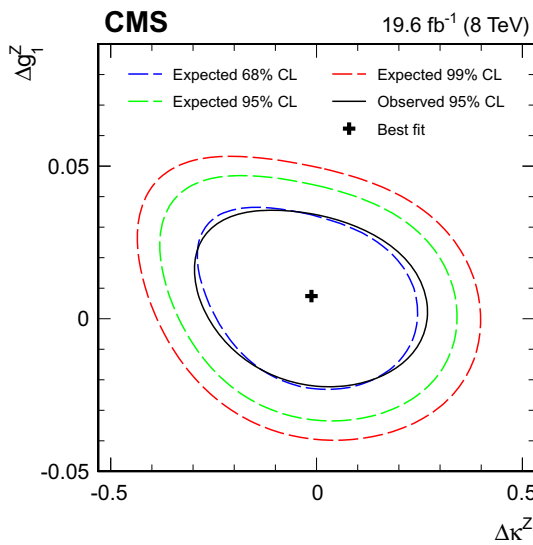
The presence of anomalous triple gauge couplings would be manifested as an increased yield of events, with the largest increase at high Z boson transverse momentum (p_T^Z). The expected p_T^Z spectrum for some aTGC values is obtained by

Table 8 One-dimensional limits on the aTGC parameters at a 95% CL for $WZ \rightarrow \ell\nu\ell'\ell'$

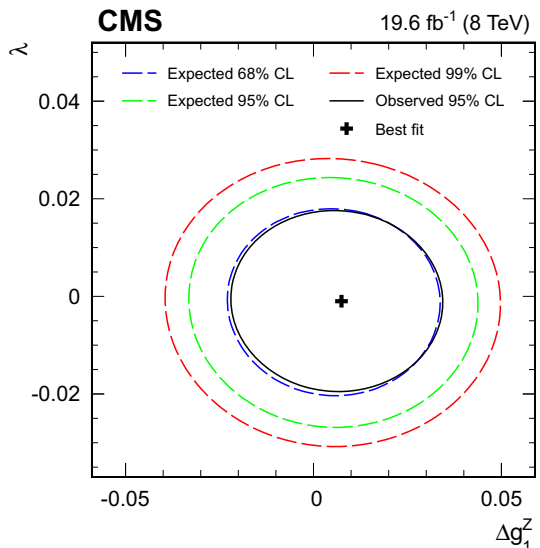
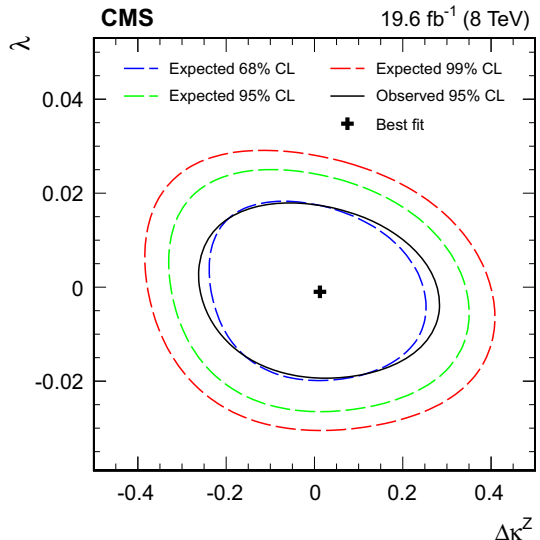
	Observed	Expected
$\Delta\kappa^Z$	[-0.21, 0.25]	[-0.29, 0.30]
Δg_1^Z	[-0.018, 0.035]	[-0.028, 0.040]
λ^Z	[-0.018, 0.016]	[-0.024, 0.021]

Table 9 One-dimensional limits on the EFT parameters at a 95% CL for $WZ \rightarrow \ell\nu\ell'\ell'$

	Observed [TeV $^{-2}$]	Expected [TeV $^{-2}$]
c_B/Λ^2	[-260, 210]	[-310, 300]
c_W/Λ^2	[-4.2, 8.0]	[-6.8, 9.2]
c_{WWW}/Λ^2	[-4.6, 4.2]	[-6.1, 5.6]

**Fig. 8** Two-dimensional observed 95% CL limits and expected 68, 95 and 99% CL limits on anomalous coupling parameters $\Delta\kappa^Z$ and Δg_1^Z

normalizing the MADGRAPH events to the expected NLO SM cross section from MCFM, and then reweighting them to the expected cross section for that particular aTGC scenario, as obtained with MCFM, based on the generated value of p_T^Z . Samples for three 2D anomalous parameter grids are generated, λ versus $\Delta\kappa^Z$, λ versus Δg_1^Z , and $\Delta\kappa^Z$ versus Δg_1^Z , where the third parameter is set to its SM value. The expected yield of the anomalous coupling signal in every p_T^Z bin is parametrized by a second-order polynomial as a function of two aTGC parameters for every channel. The observed p_T^Z spectrum is shown in Fig. 7 together with the expected spectra for a few different aTGC scenarios. A simultaneous fit to the values of aTGCs is performed [58] in all four lepton channels. A profile likelihood method, Wald gaussian approximation, and Wilks' theorem [59] are used to derive 1D and 2D limits at a 95% confidence level (CL) on each

**Fig. 9** Two-dimensional observed 95% CL limits and expected 68, 95 and 99% CL limits on anomalous coupling parameters Δg_1^Z and λ^Z **Fig. 10** Two-dimensional observed 95% CL limits and expected 68, 95 and 99% CL limits on anomalous coupling parameters $\Delta\kappa^Z$ and λ^Z

of the three aTGC parameters and every combination of two aTGC parameters, respectively, while all other parameters are set to their SM values. No significant deviation from the SM expectation is observed. Results can be found in Tables 8 and 9, and in Figs. 8, 9, and 10.

Limits on aTGC parameters were previously set by LEP [60], ATLAS [11, 14] and CMS [15]. LHC analyses using 8 TeV data are setting most stringent limits. Results in this paper show sensitivity similar to the results given by the ATLAS Collaboration in the same channel [11].

Following the calculation in Ref. [61] we find the lowest incoming parton energy for which observed limits on

Table 10 Lowest incoming partons energy for which observed limits on the coefficients would lead to unitarity violation

	\sqrt{s} [TeV]
From observed limit on c_B/Λ^2 parameter	1.6
From observed limit on c_W/Λ^2 parameter	5.1
From observed limit on c_{WWW}/Λ^2 parameter	4.3

the coefficients would lead to unitarity violation (Table 10). Overall, for charged aTGCs, we are in the region where unitarity is not violated.

8 Summary

This paper reports measurements of the WZ inclusive cross section in proton–proton collisions at $\sqrt{s} = 7$ and 8 TeV in the fully-leptonic WZ decay modes with electrons and muons in the final state. The data samples correspond to integrated luminosities of 4.9 fb^{-1} for the 7 TeV measurement and 19.6 fb^{-1} for the 8 TeV measurement. The measured production cross sections for $71 < m_Z < 111 \text{ GeV}$ are $\sigma(pp \rightarrow WZ; \sqrt{s} = 7 \text{ TeV}) = 20.14 \pm 1.32 \text{ (stat)} \pm 0.38 \text{ (theo)} \pm 1.06 \text{ (exp)} \pm 0.44 \text{ (lumi)} \text{ pb}$ and $\sigma(pp \rightarrow WZ; \sqrt{s} = 8 \text{ TeV}) = 24.09 \pm 0.87 \text{ (stat)} \pm 0.80 \text{ (theo)} \pm 1.40 \text{ (exp)} \pm 0.63 \text{ (lumi)} \text{ pb}$. These results are consistent with standard model predictions.

Using the data collected at $\sqrt{s} = 8 \text{ TeV}$, results on differential cross sections are also presented, and a search for anomalous WWZ couplings has been performed. The following one-dimensional limits at 95% CL are obtained: $-0.21 < \Delta \kappa^Z < 0.25$, $-0.018 < \Delta g_1^Z < 0.035$, and $-0.018 < \lambda^Z < 0.016$.

Acknowledgements We congratulate our colleagues in the CERN accelerator departments for the excellent performance of the LHC and thank the technical and administrative staffs at CERN and at other CMS institutes for their contributions to the success of the CMS effort. In addition, we gratefully acknowledge the computing centres and personnel of the Worldwide LHC Computing Grid for delivering so effectively the computing infrastructure essential to our analyses. Finally, we acknowledge the enduring support for the construction and operation of the LHC and the CMS detector provided by the following funding agencies: BMWFW and FWF (Austria); FNRS and FWO (Belgium); CNPq, CAPES, FAPERJ, and FAPESP (Brazil); MES (Bulgaria); CERN; CAS, MoST, and NSFC (China); COLCIENCIAS (Colombia); MSES and CSF (Croatia); RPF (Cyprus); SENESCYT (Ecuador); MoER, ERC IUT and ERDF (Estonia); Academy of Finland, MEC, and HIP (Finland); CEA and CNRS/IN2P3 (France); BMBF, DFG, and HGF (Germany); GSRT (Greece); OTKA and NIH (Hungary); DAE and DST (India); IPM (Iran); SFI (Ireland); INFN (Italy); MSIP and NRF (Republic of Korea); LAS (Lithuania); MOE and UM (Malaysia); BUAP, CINVESTAV, CONACYT, LNS, SEP, and UASLP-FAI (Mexico); MBIE (New Zealand); PAEC (Pakistan); MSHE and NSC (Poland); FCT (Portugal); JINR (Dubna); MON, RosAtom, RAS and RFBR (Russia); MESTD (Serbia); SEIDI and

CPAN (Spain); Swiss Funding Agencies (Switzerland); MST (Taipei); ThEPCenter, IPST, STAR and NSTDA (Thailand); TUBITAK and TAEK (Turkey); NASU and SFFR (Ukraine); STFC (United Kingdom); DOE and NSF (USA). Individuals have received support from the Marie-Curie programme and the European Research Council and EPLANET (European Union); the Leventis Foundation; the A. P. Sloan Foundation; the Alexander von Humboldt Foundation; the Belgian Federal Science Policy Office; the Fonds pour la Formation à la Recherche dans l’Industrie et dans l’Agriculture (FRIA-Belgium); the Agentschap voor Innovatie door Wetenschap en Technologie (IWT-Belgium); the Ministry of Education, Youth and Sports (MEYS) of the Czech Republic; the Council of Science and Industrial Research, India; the HOMING PLUS programme of the Foundation for Polish Science, cofinanced from European Union, Regional Development Fund, the Mobility Plus programme of the Ministry of Science and Higher Education, the National Science Center (Poland), contracts Harmonia 2014/14/M/ST2/00428, Opus 2013/11/B/ST2/04202, 2014/13/B/ST2/02543 and 2014/15/B/ST2/03998, Sonata-bis 2012/07/E/ST2/01406; the Thalis and Aristeia programmes cofinanced by EU-ESF and the Greek NSRF; the National Priorities Research Program by Qatar National Research Fund; the Programa Clarín-COFUND del Principado de Asturias; the Rachadapisek Sompot Fund for Postdoctoral Fellowship, Chulalongkorn University and the Chulalongkorn Academic into Its second Century Project Advancement Project (Thailand); and the Welch Foundation, contract C-1845.

Open Access This article is distributed under the terms of the Creative Commons Attribution 4.0 International License (<http://creativecommons.org/licenses/by/4.0/>), which permits unrestricted use, distribution, and reproduction in any medium, provided you give appropriate credit to the original author(s) and the source, provide a link to the Creative Commons license, and indicate if changes were made.

Funded by SCOAP³.

References

- CMS Collaboration, Measurement of Higgs boson production and properties in the WW decay channel with leptonic final states. *JHEP* **01**, 096 (2014). doi:[10.1007/JHEP01\(2014\)096](https://doi.org/10.1007/JHEP01(2014)096). arXiv:[1312.1129](https://arxiv.org/abs/1312.1129)
- CMS Collaboration, Search for new resonances decaying via WZ to leptons in proton-proton collisions at $\sqrt{s} = 8 \text{ TeV}$. *Phys. Lett. B* **740**, 83 (2015). doi:[10.1016/j.physletb.2014.11.026](https://doi.org/10.1016/j.physletb.2014.11.026). arXiv:[1407.3476](https://arxiv.org/abs/1407.3476)
- ATLAS Collaboration, Search for WZ resonances in the fully leptonic channel using pp collisions at $\sqrt{s} = 8 \text{ TeV}$ with the ATLAS detector. *Phys. Lett. B* **737**, 223 (2014). doi:[10.1016/j.physletb.2014.08.039](https://doi.org/10.1016/j.physletb.2014.08.039). arXiv:[1406.4456](https://arxiv.org/abs/1406.4456)
- CMS Collaboration, Searches for electroweak production of charginos, neutralinos, and sleptons decaying to leptons and W, Z, and Higgs bosons in pp collisions at 8 TeV. *Eur. Phys. J. C* **74**(9), 3036 (2014). doi:[10.1140/epjc/s10052-014-3036-7](https://doi.org/10.1140/epjc/s10052-014-3036-7). arXiv:[1405.7570](https://arxiv.org/abs/1405.7570)
- CMS Collaboration, Search for anomalous production of events with three or more leptons in pp collisions at $\sqrt{s} = 8 \text{ TeV}$. *Phys. Rev. D* **90**, 032006 (2014). doi:[10.1103/PhysRevD.90.032006](https://doi.org/10.1103/PhysRevD.90.032006). arXiv:[1404.5801](https://arxiv.org/abs/1404.5801)
- ATLAS Collaboration, Search for supersymmetry at $\sqrt{s} = 13 \text{ TeV}$ in final states with jets and two same-sign leptons or three leptons with the ATLAS detector. *Eur. Phys. J. C* **76**(5), 259 (2016). doi:[10.1140/epjc/s10052-016-4095-8](https://doi.org/10.1140/epjc/s10052-016-4095-8). arXiv:[1602.09058](https://arxiv.org/abs/1602.09058)
- ATLAS Collaboration, Searches for supersymmetry with the ATLAS detector using final states with two leptons and missing transverse momentum in $\sqrt{s} = 7 \text{ TeV}$ proton–proton collisions.

- Phys. Lett. B **709**, 137 (2012). doi:[10.1016/j.physletb.2012.01.076](https://doi.org/10.1016/j.physletb.2012.01.076). arXiv:[1110.6189](https://arxiv.org/abs/1110.6189)
8. DO Collaboration, A measurement of the WZ and ZZ production cross sections using leptonic final states in 8.6 fb^{-1} of $p\bar{p}$ collisions. Phys. Rev. D **85**, 112005 (2012). doi:[10.1103/PhysRevD.85.112005](https://doi.org/10.1103/PhysRevD.85.112005). arXiv:[1201.5652](https://arxiv.org/abs/1201.5652)
 9. CDF Collaboration, Measurement of the WZ cross section and triple gauge couplings in $p\bar{p}$ collisions at $\sqrt{s} = 1.96 \text{ TeV}$. Phys. Rev. D **86**, 031104 (2012). doi:[10.1103/PhysRevD.86.031104](https://doi.org/10.1103/PhysRevD.86.031104). arXiv:[1202.6629](https://arxiv.org/abs/1202.6629)
 10. ATLAS Collaboration, Measurement of WZ production in proton-proton collisions at $\sqrt{s} = 7 \text{ TeV}$ with the ATLAS detector. Eur. Phys. J. C **72**, 2173 (2012). doi:[10.1140/epjc/s10052-012-2173-0](https://doi.org/10.1140/epjc/s10052-012-2173-0). arXiv:[1208.1390](https://arxiv.org/abs/1208.1390)
 11. ATLAS Collaboration, Measurements of $W^\pm Z$ production cross sections in pp collisions at $\sqrt{s} = 8 \text{ TeV}$ with the ATLAS detector and limits on anomalous gauge boson self-couplings. Phys. Rev. D **93**, 092004 (2016). doi:[10.1103/PhysRevD.93.092004](https://doi.org/10.1103/PhysRevD.93.092004). arXiv:[1603.02151](https://arxiv.org/abs/1603.02151)
 12. ATLAS Collaboration, Measurement of the $W^\pm Z$ -boson production cross sections in pp collisions at $\sqrt{s} = 13 \text{ TeV}$ with the ATLAS detector. Phys. Lett. B **759**, 601 (2016). doi:[10.1016/j.physletb.2016.06.023](https://doi.org/10.1016/j.physletb.2016.06.023). arXiv:[1606.04017](https://arxiv.org/abs/1606.04017)
 13. CMS Collaboration, Measurement of the WZ production cross section in pp collisions at $\sqrt{s} = 13 \text{ TeV}$. Phys. Lett. B **766**, 268 (2017). doi:[10.1016/j.physletb.2017.01.011](https://doi.org/10.1016/j.physletb.2017.01.011). arXiv:[1607.06943](https://arxiv.org/abs/1607.06943)
 14. ATLAS Collaboration, Measurement of the $WW + WZ$ cross section and limits on anomalous triple gauge couplings using final states with one lepton, missing transverse momentum, and two jets with the ATLAS detector at $\sqrt{s} = 7 \text{ TeV}$. JHEP **01**, 049 (2015). doi:[10.1007/JHEP01\(2015\)049](https://doi.org/10.1007/JHEP01(2015)049). arXiv:[1410.7238](https://arxiv.org/abs/1410.7238)
 15. CMS Collaboration, Measurement of the sum of WW and WZ production with W +dijet events in pp collisions at $\sqrt{s} = 7 \text{ TeV}$. Eur. Phys. J. C **73**, 2283 (2013). doi:[10.1140/epjc/s10052-013-2283-3](https://doi.org/10.1140/epjc/s10052-013-2283-3)
 16. K.A. Olive et al., Review of particle physics. Chin. Phys. C **38**, 090001 (2014). doi:[10.1088/1674-1137/38/9/090001](https://doi.org/10.1088/1674-1137/38/9/090001)
 17. CMS Collaboration, The CMS experiment at the CERN LHC. JINST **3**, S08004 (2008). doi:[10.1088/1748-0221/3/08/S08004](https://doi.org/10.1088/1748-0221/3/08/S08004)
 18. J. Alwall et al., MadGraph 5: going beyond. JHEP **06**, 128 (2011). doi:[10.1007/JHEP06\(2011\)128](https://doi.org/10.1007/JHEP06(2011)128). arXiv:[1106.0522](https://arxiv.org/abs/1106.0522)
 19. S. Alioli, P. Nason, C. Oleari, E. Re, NLO vector-boson production matched with shower in POWHEG. JHEP **07**, 060 (2008). doi:[10.1088/1126-6708/2008/07/060](https://doi.org/10.1088/1126-6708/2008/07/060). arXiv:[0805.4802](https://arxiv.org/abs/0805.4802)
 20. P. Nason, A new method for combining NLO QCD with shower Monte Carlo algorithms. JHEP **11**, 040 (2004). doi:[10.1088/1126-6708/2004/11/040](https://doi.org/10.1088/1126-6708/2004/11/040). arXiv:[hep-ph/0409146](https://arxiv.org/abs/hep-ph/0409146)
 21. S. Frixione, P. Nason, C. Oleari, Matching NLO QCD computations with parton shower simulations: the POWHEG method. JHEP **11**, 070 (2007). doi:[10.1088/1126-6708/2007/11/070](https://doi.org/10.1088/1126-6708/2007/11/070). arXiv:[0709.2092](https://arxiv.org/abs/0709.2092)
 22. T. Bineth, N. Kauer, P. Mertsch, Gluon-induced QCD corrections to $pp \rightarrow ZZ \rightarrow \ell\ell\ell'\ell'$. In: Proceedings, 16th International Workshop on Deep Inelastic Scattering and Related Subjects (DIS 2008), p. 142. 2008. doi:[10.3360/dis.2008.142](https://doi.org/10.3360/dis.2008.142). arXiv:[0807.0024](https://arxiv.org/abs/0807.0024)
 23. J.M. Campbell, R.K. Ellis, MCFM for the tevatron and the LHC. Nucl. Phys. Proc. Suppl. **205–206**, 10 (2010). doi:[10.1016/j.nuclphysbps.2010.08.011](https://doi.org/10.1016/j.nuclphysbps.2010.08.011). arXiv:[1007.3492](https://arxiv.org/abs/1007.3492)
 24. T. Sjöstrand, S. Mrenna, P.Z. Skands, PYTHIA 6.4 physics and manual. JHEP **05**, 026 (2006). doi:[10.1088/1126-6708/2006/05/026](https://doi.org/10.1088/1126-6708/2006/05/026). arXiv:[hep-ph/0603175](https://arxiv.org/abs/hep-ph/0603175)
 25. R. Field, Early LHC underlying event data – findings and surprises. In: Hadron collider physics. Proceedings, 22nd Conference, HCP 2010, Toronto, Canada, August 23–27, 2010. arXiv:[1010.3558](https://arxiv.org/abs/1010.3558)
 26. H.-L. Lai et al., Uncertainty induced by QCD coupling in the CTEQ global analysis of parton distributions. Phys. Rev. D **82**, 054021 (2010). doi:[10.1103/PhysRevD.82.054021](https://doi.org/10.1103/PhysRevD.82.054021). arXiv:[1004.4624](https://arxiv.org/abs/1004.4624)
 27. H.-L. Lai et al., New parton distributions for collider physics. Phys. Rev. D **82**, 074024 (2010). doi:[10.1103/PhysRevD.82.074024](https://doi.org/10.1103/PhysRevD.82.074024). arXiv:[1007.2241](https://arxiv.org/abs/1007.2241)
 28. GEANT4 Collaboration, GEANT4 – a simulation toolkit. Nucl. Instrum. Methods A **506**, 250 (2003). doi:[10.1016/S0168-9002\(03\)01368-8](https://doi.org/10.1016/S0168-9002(03)01368-8)
 29. CMS Collaboration, Particle-flow event reconstruction in CMS and performance for jets, taus, and \bar{E}_T^{miss} . CMS Physics Analysis Summary CMS-PAS-PFT-09-001 (2009). <http://cdsweb.cern.ch/record/1194487>
 30. CMS Collaboration, Commissioning of the particle-flow event reconstruction with the first LHC collisions recorded in the CMS detector. CMS Physics Analysis Summary CMS-PAS-PFT-10-001, 2010. <http://cdsweb.cern.ch/record/1247373>
 31. CMS Collaboration, Performance of electron reconstruction and selection with the CMS detector in proton-proton collisions at $\sqrt{s} = 8 \text{ TeV}$. JINST **10**, P06005 (2015). doi:[10.1088/1748-0221/10/06/P06005](https://doi.org/10.1088/1748-0221/10/06/P06005)
 32. CMS Collaboration, Performance of CMS muon reconstruction in pp collision events at $\sqrt{s} = 7 \text{ TeV}$. JINST **7**, P10002 (2012). doi:[10.1088/1748-0221/7/10/P10002](https://doi.org/10.1088/1748-0221/7/10/P10002). arXiv:[1206.4071](https://arxiv.org/abs/1206.4071)
 33. M. Cacciari, G.P. Salam, Pileup subtraction using jet areas. Phys. Lett. B **659**, 119 (2008). doi:[10.1016/j.physletb.2007.09.077](https://doi.org/10.1016/j.physletb.2007.09.077). arXiv:[0707.1378](https://arxiv.org/abs/0707.1378)
 34. CMS Collaboration, Measurements of inclusive W and Z cross sections in pp collisions at $\sqrt{s} = 7 \text{ TeV}$. JHEP **01**, 080 (2011). doi:[10.1007/JHEP01\(2011\)080](https://doi.org/10.1007/JHEP01(2011)080)
 35. M. Cacciari, G.P. Salam, G. Soyez, The anti- k_t jet clustering algorithm. JHEP **04**, 063 (2008). doi:[10.1088/1126-6708/2008/04/063](https://doi.org/10.1088/1126-6708/2008/04/063). arXiv:[0802.1189](https://arxiv.org/abs/0802.1189)
 36. M. Cacciari, G.P. Salam, G. Soyez, FastJet user manual. Eur. Phys. J. C **72**, 1896 (2012). doi:[10.1140/epjc/s10052-012-1896-2](https://doi.org/10.1140/epjc/s10052-012-1896-2). arXiv:[1111.6097](https://arxiv.org/abs/1111.6097)
 37. CMS Collaboration, Determination of jet energy calibration and transverse momentum resolution in CMS. JINST **6**, P11002 (2011). doi:[10.1088/1748-0221/6/11/P11002](https://doi.org/10.1088/1748-0221/6/11/P11002). arXiv:[1107.4277](https://arxiv.org/abs/1107.4277)
 38. CMS Collaboration, Measurement of WW production and search for the Higgs boson in pp collisions at $\sqrt{s} = 7 \text{ TeV}$. Phys. Lett. B **699**, 25 (2011). doi:[10.1016/j.physletb.2011.03.056](https://doi.org/10.1016/j.physletb.2011.03.056). arXiv:[1102.5429](https://arxiv.org/abs/1102.5429)
 39. J.M. Campbell, J.W. Huston, W.J. Stirling, Hard interactions of quarks and gluons: a primer for LHC physics. Rep. Prog. Phys. **70**, 89 (2007). doi:[10.1088/0034-4885/70/1/R02](https://doi.org/10.1088/0034-4885/70/1/R02). arXiv:[hep-ph/0611148](https://arxiv.org/abs/hep-ph/0611148)
 40. CMS Collaboration, Measurement of the inelastic proton–proton cross section at $\sqrt{s} = 7 \text{ TeV}$. Phys. Lett. B **722**, 5 (2013). doi:[10.1016/j.physletb.2013.03.024](https://doi.org/10.1016/j.physletb.2013.03.024)
 41. CMS Collaboration, Measurement of the ZZ production cross section and search for anomalous couplings in $2\ell 2\ell'$ final states in pp collisions at $\sqrt{s} = 7 \text{ TeV}$. JHEP **01**, 063 (2013). doi:[10.1007/JHEP01\(2013\)063](https://doi.org/10.1007/JHEP01(2013)063)
 42. CMS Collaboration, Measurement of the W^+W^- and ZZ production cross sections in pp collisions at $\sqrt{s} = 8 \text{ TeV}$. Phys. Lett. B **721**, 190 (2013). doi:[10.1016/j.physletb.2013.03.027](https://doi.org/10.1016/j.physletb.2013.03.027)
 43. CMS Collaboration, Measurement of the $W\gamma$ and $W\gamma$ inclusive cross sections in pp collisions at $\sqrt{s} = 7 \text{ TeV}$ and limits on anomalous triple gauge boson couplings. Phys. Rev. D **89**, 092005 (2014). doi:[10.1103/PhysRevD.89.092005](https://doi.org/10.1103/PhysRevD.89.092005)
 44. CMS Collaboration, Measurement of the $Z\gamma$ production cross section in pp collisions at 8 TeV and search for anomalous triple gauge boson couplings. JHEP **04**, 164 (2015). doi:[10.1007/JHEP04\(2015\)164](https://doi.org/10.1007/JHEP04(2015)164). arXiv:[1502.05664](https://arxiv.org/abs/1502.05664)
 45. CMS Collaboration, Measurement of top quark-antiquark pair production in association with a W or Z boson in pp collisions at $\sqrt{s} = 8 \text{ TeV}$. Eur. Phys. J. C **74**, 3060 (2014). doi:[10.1140/epjc/s10052-014-3060-7](https://doi.org/10.1140/epjc/s10052-014-3060-7)

46. CMS Collaboration, Absolute calibration of the luminosity measurement at CMS: winter 2012 update. CMS Physics Analysis Summary CMS-PAS-SMP-12-008 (2012). <http://cdsweb.cern.ch/record/1434360>
47. CMS Collaboration, CMS luminosity based on pixel cluster counting - summer 2013 update. CMS Physics Analysis Summary CMS-PAS-LUM-13-001 (2013). <http://cdsweb.cern.ch/record/1598864>
48. L. Lyons, D. Gibaut, P. Clifford, How to combine correlated estimates of a single physical quantity. Nucl. Instrum. Methods A **270**, 110 (1988). doi:[10.1016/0168-9002\(88\)90018-6](https://doi.org/10.1016/0168-9002(88)90018-6)
49. M. Grazzini, S. Kallweit, D. Rathlev, M. Wiesemann, $W^\pm Z$ production at hadron colliders in NNLO QCD. Phys. Lett. B **761**, 179 (2016). doi:[10.1016/j.physletb.2016.08.017](https://doi.org/10.1016/j.physletb.2016.08.017). arXiv:[1604.08576](https://arxiv.org/abs/1604.08576)
50. G. D'Agostini, A multidimensional unfolding method based on Bayes' theorem. Nucl. Instrum. Methods A **362**, 487 (1995). doi:[10.1016/0168-9002\(95\)00274-X](https://doi.org/10.1016/0168-9002(95)00274-X)
51. T. Adye, Unfolding algorithms and tests using RooUnfold. In PHYSTAT 2011 Workshop on Statistical Issues Related to Discovery Claims in Search Experiments and Unfolding, ed. by H. Prosper, L. Lyons, (Geneva, Switzerland, 2011) p. 313. arXiv:[1105.1160](https://arxiv.org/abs/1105.1160). DOI: 10.5170/CERN-2011-006.313
52. A. Valasssi, Combining correlated measurements of several different physical quantities. Nucl. Instrum. Methods A **500**, 391 (2003). doi:[10.1016/S0168-9002\(03\)00329-2](https://doi.org/10.1016/S0168-9002(03)00329-2)
53. K. Hagiwara, R.D. Peccei, D. Zeppenfeld, Probing the weak boson sector in $e^+e^- \rightarrow W^+W^-$. Nucl. Phys. B **282**, 253 (1987). doi:[10.1016/0550-3213\(87\)90685-7](https://doi.org/10.1016/0550-3213(87)90685-7)
54. K. Hagiwara, J. Woodside, D. Zeppenfeld, Measuring the WWZ coupling at the fermilab tevatron. Phys. Rev. D **41**, 2113 (1990). doi:[10.1103/PhysRevD.41.2113](https://doi.org/10.1103/PhysRevD.41.2113)
55. C. Grosse-Knetter, I. Kuss, D. Schildknecht, Nonstandard gauge boson selfinteractions within a gauge invariant model. Z. Phys. C **60**, 375 (1993). doi:[10.1007/BF01474637](https://doi.org/10.1007/BF01474637). arXiv:[hep-ph/9304281](https://arxiv.org/abs/hep-ph/9304281)
56. M.S. Bilenky, J.L. Kneur, F.M. Renard, D. Schildknecht, Trilinear couplings among the electroweak vector bosons and their determination at LEP-200. Nucl. Phys. B **409**, 22 (1993). doi:[10.1016/0550-3213\(93\)90445-U](https://doi.org/10.1016/0550-3213(93)90445-U)
57. M.S. Bilenky, J.-L. Kneur, F.M. Renard, D. Schildknecht, The potential of a new linear collider for the measurement of the trilinear couplings among the electroweak vector bosons. Nucl. Phys. B **419**, 240 (1994). doi:[10.1016/0550-3213\(94\)90041-8](https://doi.org/10.1016/0550-3213(94)90041-8). arXiv:[hep-ph/9312202](https://arxiv.org/abs/hep-ph/9312202)
58. ATLAS and CMS Collaborations and LHC Higgs Combination Group, Procedure for the LHC Higgs boson search combination in Summer 2011, CMS NOTE CMS-NOTE-2011-005, ATL-PHYS-PUB-2011-11, CERN, Geneva (2011). <http://cds.cern.ch/record/1379837>
59. G. Cowan, K. Cranmer, E. Gross, O. Vitells, Asymptotic formulae for likelihood-based tests of new physics. Eur. Phys. J. C **71**, 1554 (2011). doi:[10.1140/epjc/s10052-011-1554-0](https://doi.org/10.1140/epjc/s10052-011-1554-0). arXiv:[1007.1727](https://arxiv.org/abs/1007.1727)
60. The ALEPH Collaboration, The DELPHI Collaboration, The L3 Collaboration, The OPAL Collaboration, The LEP Electroweak Working Group, Electroweak measurements in electron-positron collisions at W-boson-pair energies at LEP. Phys. Rept. **532**, 119 (2013). doi:[10.1016/j.physrep.2013.07.004](https://doi.org/10.1016/j.physrep.2013.07.004). arXiv:[1302.3415](https://arxiv.org/abs/1302.3415)
61. T. Corbett, O.J.P. Eboli, M.C. Gonzalez-Garcia, Unitarity constraints on dimension-six operators. Phys. Rev. D **91**, 035014 (2015). doi:[10.1103/PhysRevD.91.035014](https://doi.org/10.1103/PhysRevD.91.035014). arXiv:[1411.5026](https://arxiv.org/abs/1411.5026)

CMS Collaboration

Yerevan Physics Institute, Yerevan, Armenia

V. Khachatryan, A. M. Sirunyan, A. Tumasyan

Institut für Hochenergiephysik der OeAW, Wien, Austria

W. Adam, E. Asilar, T. Bergauer, J. Brandstetter, E. Brondolin, M. Dragicevic, J. Erö, M. Flechl, M. Friedl, R. Frühwirth¹, V. M. Ghete, C. Hartl, N. Hörmann, J. Hrubec, M. Jeitler¹, A. König, I. Krätschmer, D. Liko, T. Matsushita, I. Mikulec, D. Rabady, N. Rad, B. Rahbaran, H. Rohringer, J. Schieck¹, J. Strauss, W. Treberer-Treberspurg, W. Waltenberger, C.-E. Wulz¹

National Centre for Particle and High Energy Physics, Minsk, Belarus

V. Mossolov, N. Shumeiko, J. Suarez Gonzalez

Universiteit Antwerpen, Antwerp, Belgium

S. Alderweireldt, E. A. De Wolf, X. Janssen, J. Lauwers, M. Van De Klundert, H. Van Haevermaet, P. Van Mechelen, N. Van Remortel, A. Van Spilbeeck

Vrije Universiteit Brussel, Brussels, Belgium

S. Abu Zeid, F. Blekman, J. D'Hondt, N. Daci, I. De Bruyn, K. Deroover, N. Heracleous, S. Lowette, S. Moortgat, L. Moreels, A. Olbrechts, Q. Python, S. Tavernier, W. Van Doninck, P. Van Mulders, I. Van Parijs

Université Libre de Bruxelles, Brussels, Belgium

H. Brun, C. Caillol, B. Clerbaux, G. De Lentdecker, H. Delannoy, G. Fasanella, L. Favart, R. Goldouzian, A. Grebenyuk, G. Karapostoli, T. Lenzi, A. Léonard, J. Luetic, T. Maerschalk, A. Marinov, A. Randle-conde, T. Seva, C. Vander Velde, P. Vanlaer, R. Yonamine, F. Zenoni, F. Zhang²

Ghent University, Ghent, Belgium

A. Cimmino, T. Cornelis, D. Dobur, A. Fagot, G. Garcia, M. Gul, D. Poyraz, S. Salva, R. Schöfbeck, M. Tytgat, W. Van Driessche, E. Yazgan, N. Zaganidis

Université Catholique de Louvain, Louvain-la-Neuve, Belgium

H. Bakhshiansohi, C. Beluffi³, O. Bondu, S. Brochet, G. Bruno, A. Caudron, S. De Visscher, C. Delaere, M. Delcourt, L. Forthomme, B. Francois, A. Giannanco, A. Jafari, P. Jez, M. Komm, V. Lemaitre, A. Magitteri, A. Mertens, M. Musich, C. Nuttens, K. Piotrzkowski, L. Quertenmont, M. Selvaggi, M. Vidal Marono, S. Wertz

Université de Mons, Mons, Belgium

N. Belyi

Centro Brasileiro de Pesquisas Fisicas, Rio de Janeiro, Brazil

W. L. Aldá Júnior, F. L. Alves, G. A. Alves, L. Brito, C. Hensel, A. Moraes, M. E. Pol, P. Rebello Teles

Universidade do Estado do Rio de Janeiro, Rio de Janeiro, Brazil

E. Belchior Batista Das Chagas, W. Carvalho, J. Chinellato⁴, A. Custódio, E. M. Da Costa, G. G. Da Silveira⁵, D. De Jesus Damiao, C. De Oliveira Martins, S. Fonseca De Souza, L. M. Huertas Guativa, H. Malbouisson, D. Matos Figueiredo, C. Mora Herrera, L. Mundim, H. Nogima, W. L. Prado Da Silva, A. Santoro, A. Sznajder, E. J. Tonelli Manganote⁴, A. Vilela Pereira

Universidade Estadual Paulista^a, Universidade Federal do ABC^b, São Paulo, Brazil

S. Ahuja^a, C. A. Bernardes^b, S. Dogra^a, T. R. Fernandez Perez Tomei^a, E. M. Gregores^b, P. G. Mercadante^b, C. S. Moon^a, S. F. Novaes^a, Sandra S. Padula^a, D. Romero Abad^b, J. C. Ruiz Vargas

Institute for Nuclear Research and Nuclear Energy, Sofia, Bulgaria

A. Aleksandrov, R. Hadjiiska, P. Iaydjiev, M. Rodozov, S. Stoykova, G. Sultanov, M. Vutova, J. Duarte⁶

University of Sofia, Sofia, Bulgaria

A. Dimitrov, I. Glushkov, L. Litov, B. Pavlov, P. Petkov

Beihang University, Beijing, China

W. Fang⁶

Institute of High Energy Physics, Beijing, China

M. Ahmad, J. G. Bian, G. M. Chen, H. S. Chen, M. Chen, Y. Chen⁷, T. Cheng, C. H. Jiang, D. Leggat, Z. Liu, F. Romeo, S. M. Shaheen, A. Spiezia, J. Tao, C. Wang, Z. Wang, H. Zhang, J. Zhao

State Key Laboratory of Nuclear Physics and Technology, Peking University, Beijing, China

Y. Ban, G. Chen, Q. Li, S. Liu, Y. Mao, S. J. Qian, D. Wang, Z. Xu

Universidad de Los Andes, Bogotá, Colombia

C. Avila, A. Cabrera, L. F. Chaparro Sierra, C. Florez, J. P. Gomez, C. F. González Hernández, J. D. Ruiz Alvarez, J. C. Sanabria

Faculty of Electrical Engineering, Mechanical Engineering and Naval Architecture, University of Split, Split, Croatia

N. Godinovic, D. Lelas, I. Puljak, P. M. Ribeiro Cipriano

Faculty of Science, University of Split, Split, Croatia

Z. Antunovic, M. Kovac

Institute Rudjer Boskovic, Zagreb, Croatia

V. Brigljevic, D. Ferencek, K. Kadija, S. Micanovic, L. Sudic, T. Susa

University of Cyprus, Nicosia, Cyprus

A. Attikis, G. Mavromanolakis, J. Mousa, C. Nicolaou, F. Ptochos, P. A. Razis, H. Rykaczewski

Charles University, Prague, Czech Republic

M. Finger⁸, M. Finger Jr.⁸

Universidad San Francisco de Quito, Quito, Ecuador

E. Carrera Jarrin

Academy of Scientific Research and Technology of the Arab Republic of Egypt, Egyptian Network of High Energy Physics, Cairo, Egypt

S. Elgammal⁹, A. Mohamed¹⁰, E. Salama^{9,11}

National Institute of Chemical Physics and Biophysics, Tallinn, Estonia

B. Calpas, M. Kadastik, M. Murumaa, L. Perrini, M. Raidal, A. Tiko, C. Veelken

Department of Physics, University of Helsinki, Helsinki, Finland

P. Eerola, J. Pekkanen, M. Voutilainen

Helsinki Institute of Physics, Helsinki, Finland

J. Häkkinen, V. Karimäki, R. Kinnunen, T. Lampén, K. Lassila-Perini, S. Lehti, T. Lindén, P. Luukka, T. Peltola, J. Tuominiemi, E. Tuovinen, L. Wendland

Lappeenranta University of Technology, Lappeenranta, Finland

J. Talvitie, T. Tuuva

IRFU, CEA, Université Paris-Saclay, Gif-sur-Yvette, France

M. Besancon, F. Couderc, M. Dejardin, D. Denegri, B. Fabbro, J. L. Faure, C. Favaro, F. Ferri, S. Ganjour, S. Ghosh, A. Givernaud, P. Gras, G. Hamel de Monchenault, P. Jarry, I. Kucher, E. Locci, M. Machet, J. Malcles, J. Rander, A. Rosowsky, M. Titov, A. Zghiche

Laboratoire Leprince-Ringuet, Ecole Polytechnique, IN2P3-CNRS, Palaiseau, France

A. Abdulsalam, I. Antropov, S. Baffioni, F. Beaudette, P. Busson, L. Cadamuro, E. Chapon, C. Charlot, O. Davignon, R. Granier de Cassagnac, M. Jo, S. Lisniak, P. Miné, M. Nguyen, C. Ochando, G. Ortona, P. Paganini, P. Pigard, S. Regnard, R. Salerno, Y. Sirois, T. Strebler, Y. Yilmaz, A. Zabi

Institut Pluridisciplinaire Hubert Curien, Université de Strasbourg, Université de Haute Alsace Mulhouse, CNRS/IN2P3, Strasbourg, France

J.-L. Agram¹², J. Andrea, A. Aubin, D. Bloch, J.-M. Brom, M. Buttignol, E. C. Chabert, N. Chanon, C. Collard, E. Conte¹², X. Coubez, J.-C. Fontaine¹², D. Gelé, U. Goerlach, A.-C. Le Bihan, J. A. Merlin¹³, K. Skovpen, P. Van Hove

Centre de Calcul de l’Institut National de Physique Nucléaire et de Physique des Particules, CNRS/IN2P3, Villeurbanne, France

S. Gadrat

Université de Lyon, Université Claude Bernard Lyon 1, CNRS-IN2P3, Institut de Physique Nucléaire de Lyon, Villeurbanne, France

S. Beauceron, C. Bernet, G. Boudoul, E. Bouvier, C. A. Carrillo Montoya, R. Chierici, D. Contardo, B. Courbon, P. Depasse, H. El Mamouni, J. Fan, J. Fay, S. Gascon, M. Gouzevitch, G. Grenier, B. Ille, F. Lagarde, I. B. Laktineh, M. Lethuillier, L. Mirabito, A. L. Pequegnot, S. Perries, A. Popov¹⁴, D. Sabes, V. Sordini, M. Vander Donckt, P. Verdier, S. Viret

Georgian Technical University, Tbilisi, Georgia

T. Toriashvili¹⁵

Tbilisi State University, Tbilisi, Georgia

Z. Tsamalaidze⁸

RWTH Aachen University, I. Physikalisches Institut, Aachen, Germany

C. Autermann, S. Beranek, L. Feld, A. Heister, M. K. Kiesel, K. Klein, M. Lipinski, A. Ostapchuk, M. Preuten, F. Raupach, S. Schael, C. Schomakers, J. F. Schulte, J. Schulz, T. Verlage, H. Weber, V. Zhukov¹⁴

RWTH Aachen University, III. Physikalisches Institut A, Aachen, Germany

M. Brodski, E. Dietz-Laursonn, D. Duchardt, M. Endres, M. Erdmann, S. Erdweg, T. Esch, R. Fischer, A. Güth, M. Hamer, T. Hebbeker, C. Heidemann, K. Hoepfner, S. Knutzen, M. Merschmeyer, A. Meyer, P. Millet, S. Mukherjee, M. Olschewski, K. Padéken, T. Pook, M. Radziej, H. Reithler, M. Rieger, F. Scheuch, L. Sonnenschein, D. Teyssier, S. Thüer

RWTH Aachen University, III. Physikalisches Institut B, Aachen, Germany

V. Cherepanov, G. Flügge, W. Haj Ahmad, F. Hoehle, B. Kargoll, T. Kress, A. Künsken, J. Lingemann, A. Nehrkorn, A. Nowack, I. M. Nugent, C. Pistone, O. Pooth, A. Stahl¹³

Deutsches Elektronen-Synchrotron, Hamburg, Germany

M. Aldaya Martin, C. Asawatangtrakuldee, K. Beernaert, O. Behnke, U. Behrens, A. A. Bin Anuar, K. Borras¹⁶, A. Campbell, P. Connor, C. Contreras-Campana, F. Costanza, C. Diez Pardos, G. Dolinska, G. Eckerlin, D. Eckstein, E. Eren, E. Gallo¹⁷, J. Garay Garcia, A. Geiser, A. Gzhko, J. M. Grados Luyando, P. Gunnellini, A. Harb, J. Hauk, M. Hempel¹⁸, H. Jung, A. Kalogeropoulos, O. Karacheban¹⁸, M. Kasemann, J. Keaveney, J. Kieseler, C. Kleinwort, I. Korol, D. Krücker, W. Lange, A. Lelek, J. Leonard, K. Lipka, A. Lobanov, W. Lohmann¹⁸, R. Mankel, I.-A. Melzer-Pellmann, A. B. Meyer, G. Mittag, J. Mnich, A. Mussgiller, E. Ntomari, D. Pitzl, R. Placakyte, A. Raspereza, B. Roland, M. Ö. Sahin, P. Saxena, T. Schoerner-Sadenius, C. Seitz, S. Spannagel, N. Stefanik, K. D. Trippkewitz, G. P. Van Onsem, R. Walsh, C. Wissing

University of Hamburg, Hamburg, Germany

V. Blobel, M. Centis Vignal, A. R. Draeger, T. Dreyer, E. Garutti, K. Goebel, D. Gonzalez, J. Haller, M. Hoffmann, A. Junkes, R. Klanner, R. Kogler, N. Kovalchuk, T. Lapsien, T. Lenz, I. Marchesini, D. Marconi, M. Meyer, M. Niedziela, D. Nowatschin, J. Ott, F. Pantaleo¹³, T. Peiffer, A. Perieanu, J. Poehlsen, C. Sander, C. Scharf, P. Schleper, A. Schmidt, S. Schumann, J. Schwandt, H. Stadie, G. Steinbrück, F. M. Stober, M. Stöver, H. Tholen, D. Troendle, E. Usai, L. Vanelderen, A. Vanhoefer, B. Vormwald

Institut für Experimentelle Kernphysik, Karlsruhe, Germany

C. Barth, C. Baus, J. Berger, E. Butz, T. Chwalek, F. Colombo, W. De Boer, A. Dierlamm, S. Fink, R. Friese, M. Giffels, A. Gilbert, P. Goldenzweig, D. Haitz, F. Hartmann¹³, S. M. Heindl, U. Husemann, I. Katkov¹⁴, P. Lobelle Pardo, B. Maier, H. Mildner, M. U. Mozer, T. Müller, Th. Müller, M. Plagge, G. Quast, K. Rabbertz, S. Röcker, F. Roscher, M. Schröder, I. Shvetsov, G. Sieber, H. J. Simonis, R. Ulrich, J. Wagner-Kuhr, S. Wayand, M. Weber, T. Weiler, S. Williamson, C. Wöhrmann, R. Wolf

Institute of Nuclear and Particle Physics (INPP), NCSR Demokritos, Aghia Paraskevi, Greece

G. Anagnostou, G. Daskalakis, T. Geralis, V. A. Giakoumopoulou, A. Kyriakis, D. Loukas, I. Topsis-Giotis

National and Kapodistrian University of Athens, Athens, Greece

A. Agapitos, S. Kesisoglou, A. Panagiotou, N. Saoulidou, E. Tziaferi

University of Ioánnina, Ioannina, Greece

I. Evangelou, G. Flouris, C. Foudas, P. Kokkas, N. Loukas, N. Manthos, I. Papadopoulos, E. Paradas

MTA-ELTE Lendület CMS Particle and Nuclear Physics Group, Eötvös Loránd University, Budapest, Hungary

N. Filipovic

Wigner Research Centre for Physics, Budapest, Hungary

G. Bencze, C. Hajdu, P. Hidas, D. Horvath¹⁹, F. Sikler, V. Veszpremi, G. Vesztergombi²⁰, A. J. Zsigmond

Institute of Nuclear Research ATOMKI, Debrecen, Hungary

N. Beni, S. Czellar, J. Karancsi²¹, A. Makovec, J. Molnar, Z. Szillasi

University of Debrecen, Debrecen, Hungary

M. Bartók²⁰, P. Raics, Z. L. Trocsanyi, B. Ujvari

National Institute of Science Education and Research, Bhubaneswar, India

S. Bahinipati, S. Choudhury²², P. Mal, K. Mandal, A. Nayak²³, D. K. Sahoo, N. Sahoo, S. K. Swain

Punjab University, Chandigarh, India

S. Bansal, S. B. Beri, V. Bhatnagar, R. Chawla, U. Bhawandeep, A. K. Kalsi, A. Kaur, M. Kaur, R. Kumar, A. Mehta, M. Mittal, J. B. Singh, G. Walia

University of Delhi, Delhi, India

Ashok Kumar, A. Bhardwaj, B. C. Choudhary, R. B. Garg, S. Keshri, S. Malhotra, M. Naimuddin, N. Nishu, K. Ranjan, R. Sharma, V. Sharma

Saha Institute of Nuclear Physics, Kolkata, India

R. Bhattacharya, S. Bhattacharya, K. Chatterjee, S. Dey, S. Dutt, S. Dutta, S. Ghosh, N. Majumdar, A. Modak, K. Mondal, S. Mukhopadhyay, S. Nandan, A. Purohit, A. Roy, D. Roy, S. Roy Chowdhury, S. Sarkar, M. Sharan, S. Thakur

Indian Institute of Technology Madras, Madras, India

P. K. Behera

Bhabha Atomic Research Centre, Mumbai, IndiaR. Chudasama, D. Dutta, V. Jha, V. Kumar, A. K. Mohanty¹³, P. K. Netrakanti, L. M. Pant, P. Shukla, A. Topkar**Tata Institute of Fundamental Research-A, Mumbai, India**

T. Aziz, S. Dugad, G. Kole, B. Mahakud, S. Mitra, G. B. Mohanty, B. Parida, N. Sur, B. Sutar

Tata Institute of Fundamental Research-B, Mumbai, IndiaS. Banerjee, S. Bhownik²⁴, R. K. Dewanjee, S. Ganguly, M. Guchait, Sa. Jain, S. Kumar, M. Maity²⁴, G. Majumder, K. Mazumdar, T. Sarkar²⁴, N. Wickramage²⁵**Indian Institute of Science Education and Research (IISER), Pune, India**

S. Chauhan, S. Dube, V. Hegde, A. Kapoor, K. Kotekar, A. Rane, S. Sharma

Institute for Research in Fundamental Sciences (IPM), Tehran, IranH. Behnamian, S. Chenaranian²⁶, E. Eskandari Tadavani, S. M. Etesami²⁶, A. Fahim²⁷, M. Khakzad, M. Mohammadi Najafabadi, M. Naseri, S. Pakhtinat Mehdiabadi, F. Rezaei Hosseiniabadi, B. Safarzadeh²⁸, M. Zeinali**University College Dublin, Dublin, Ireland**

M. Felcini, M. Grunewald

INFN Sezione di Bari^a, Università di Bari^b, Politecnico di Bari^c, Bari, ItalyM. Abbrescia^{a,b}, C. Calabria^{a,b}, C. Caputo^{a,b}, A. Colaleo^a, D. Creanza^{a,c}, L. Cristella^{a,b}, N. De Filippis^{a,c}, M. De Palma^{a,b}, L. Fiore^a, G. Iaselli^{a,c}, G. Maggi^{a,c}, M. Maggi^a, G. Miniello^{a,b}, S. My^{a,b}, S. Nuzzo^{a,b}, A. Pompili^{a,b}, G. Pugliese^{a,c}, R. Radogna^{a,b}, A. Ranieri^a, G. Selvaggi^{a,b}, L. Silvestris^{a,13}, R. Venditti^{a,b}, P. Verwilligen^a**INFN Sezione di Bologna^a, Università di Bologna^b, Bologna, Italy**G. Abbiendi^a, C. Battilana, D. Bonacorsi^{a,b}, S. Braibant-Giacomelli^{a,b}, L. Brigliadori^{a,b}, R. Campanini^{a,b}, P. Capiluppi^{a,b}, A. Castro^{a,b}, F. R. Cavallo^a, S. S. Chhibra^{a,b}, G. Codispoti^{a,b}, M. Cuffiani^{a,b}, G. M. Dallavalle^a, F. Fabbri^a, A. Fanfani^{a,b}, D. Fasanella^{a,b}, P. Giacomelli^a, C. Grandi^a, L. Guiducci^{a,b}, S. Marcellini^a, G. Masetti^a, A. Montanari^a, F. L. Navarria^{a,b}, A. Perrotta^a, A. M. Rossi^{a,b}, T. Rovelli^{a,b}, G. P. Siroli^{a,b}, N. Tosi^{a,b,13}**INFN Sezione di Catania^a, Università di Catania^b, Catania, Italy**S. Albergo^{a,b}, M. Chiorboli^{a,b}, S. Costa^{a,b}, A. Di Mattia^a, F. Giordano^{a,b}, R. Potenza^{a,b}, A. Tricomi^{a,b}, C. Tuve^{a,b}**INFN Sezione di Firenze^a, Università di Firenze^b, Florence, Italy**G. Barbagli^a, V. Ciulli^{a,b}, C. Civinini^a, R. D'Alessandro^{a,b}, E. Focardi^{a,b}, V. Gori^{a,b}, P. Lenzi^{a,b}, M. Meschini^a, S. Paoletti^a, G. Sguazzoni^a, L. Viliani^{a,b,13}**INFN Laboratori Nazionali di Frascati, Frascati, Italy**L. Benussi, S. Bianco, F. Fabbri, D. Piccolo, F. Primavera¹³**INFN Sezione di Genova^a, Università di Genova^b, Genoa, Italy**V. Calvelli^{a,b}, F. Ferro^a, M. Lo Vetere^{a,b}, M. R. Monge^{a,b}, E. Robutti^a, S. Tosi^{a,b}**INFN Sezione di Milano-Bicocca^a, Università di Milano-Bicocca^b, Milan, Italy**L. Brianza¹³, M. E. Dinardo^{a,b}, S. Fiorendi^{a,b}, S. Gennai^a, A. Ghezzi^{a,b}, P. Govoni^{a,b}, S. Malvezzi^a, R. A. Manzoni^{a,b,13}, B. Marzocchi^{a,b}, D. Menasce^a, L. Moroni^a, M. Paganoni^{a,b}, D. Pedrinia^a, S. Pigazzini, S. Ragazzi^{a,b}, T. Tabarelli de Fatis^{a,b}**INFN Sezione di Napoli^a, Università di Napoli 'Federico II'^b Naples, Italy, Università della Basilicata^c, Potenza, Italy, Università G. Marconi^d, Rome, Italy**S. Buontempo^a, N. Cavallo^{a,c}, G. De Nardo, S. Di Guida^{a,d,13}, M. Esposito^{a,b}, F. Fabozzi^{a,c}, A. O. M. Iorio^{a,b}, G. Lanza^a, L. Lista^a, S. Meola^{a,d,13}, P. Paolucci^{a,13}, C. Sciacca^{a,b}, F. Thyssen

INFN Sezione di Padova^a, Università di Padova^b, Padua, Italy, Università di Trento^c, Trento, Italy

P. Azzi^{a,13}, N. Bacchetta^a, L. Benato^{a,b}, D. Bisello^{a,b}, A. Boletti^{a,b}, R. Carlin^{a,b}, A. Carvalho Antunes De Oliveira^{a,b}, P. Checchia^a, M. Dall'Osso^{a,b}, P. De Castro Manzano^a, T. Dorigo^a, U. Dosselli^a, F. Gasparini^{a,b}, U. Gasparini^{a,b}, A. Gozzelino^a, S. Lacaprara^a, M. Margoni^{a,b}, A. T. Meneguzzo^{a,b}, J. Pazzini^{a,b,13}, N. Pozzobon^{a,b}, P. Ronchese^{a,b}, F. Simonetto^{a,b}, E. Torassa^a, M. Zanetti, P. Zotto^{a,b}, A. Zucchetta^{a,b}, G. Zumerle^{a,b}

INFN Sezione di Pavia^a, Università di Pavia^b, Pavia, Italy

A. Braghieri^a, A. Magnani^{a,b}, P. Montagna^{a,b}, S. P. Ratti^{a,b}, V. Re^a, C. Riccardi^{a,b}, P. Salvini^a, I. Vai^{a,b}, P. Vitulo^{a,b}

INFN Sezione di Perugia^a, Università di Perugia^b, Perugia, Italy

L. Alunni Solestizi^{a,b}, G. M. Bilei^a, D. Ciangottini^{a,b}, L. Fanò^{a,b}, P. Lariccia^{a,b}, R. Leonardi^{a,b}, G. Mantovani^{a,b}, M. Menichelli^a, A. Saha^a, A. Santocchia^{a,b}

INFN Sezione di Pisa^a, Università di Pisa^b, Scuola Normale Superiore di Pisa^c, Pisa, Italy

K. Androsov^{a,29}, P. Azzurri^{a,13}, G. Bagliesi^a, J. Bernardini^a, T. Boccali^a, R. Castaldi^a, M. A. Ciocci^{a,29}, R. Dell'Orso^a, S. Donato^{a,c}, G. Fedi, A. Giassi^a, M. T. Grippo^{a,29}, F. Ligabue^{a,c}, T. Lomidze^a, L. Martini^{a,b}, A. Messineo^{a,b}, F. Palla^a, A. Rizzi^{a,b}, A. Savoy-Navarro^{a,30}, P. Spagnolo^a, R. Tenchini^a, G. Tonelli^{a,b}, A. Venturi^a, P. G. Verdini^a

INFN Sezione di Roma^a, Università di Roma^b, Rome, Italy

L. Barone^{a,b}, F. Cavallari^a, M. Cipriani^{a,b}, G. D'imperio^{a,b,13}, D. Del Re^{a,b,13}, M. Diemoz^a, S. Gelli^{a,b}, C. Jorda^a, E. Longo^{a,b}, F. Margaroli^{a,b}, P. Meridiani^a, G. Organtini^{a,b}, R. Paramatti^a, F. Preiato^{a,b}, S. Rahatlou^{a,b}, C. Rovelli^a, F. Santanastasio^{a,b}

INFN Sezione di Torino^a, Università di Torino^b, Turin, Italy, Università del Piemonte Orientale^c, Novara, Italy

N. Amapane^{a,b}, R. Arcidiacono^{a,c,13}, S. Argiro^{a,b}, M. Arneodo^{a,c}, N. Bartosik^a, R. Bellan^{a,b}, C. Biino^a, N. Cartiglia^a, F. Cenna^{a,b}, M. Costa^{a,b}, R. Covarelli^{a,b}, A. Degano^{a,b}, N. Demaria^a, L. Finco^{a,b}, B. Kiani^{a,b}, C. Mariotti^a, S. Maselli^a, E. Migliore^{a,b}, V. Monaco^{a,b}, E. Monteil^{a,b}, M. M. Obertino^{a,b}, L. Pacher^{a,b}, N. Pastrone^a, M. Pelliccioni^a, G. L. Pinna Angioni^{a,b}, F. Ravera^{a,b}, A. Romero^{a,b}, M. Ruspa^{a,c}, R. Sacchi^{a,b}, K. Shchelina^{a,b}, V. Sola^a, A. Solano^{a,b}, A. Staiano^a, P. Traczyk^{a,b}

INFN Sezione di Trieste^a, Università di Trieste^b, Trieste, Italy

S. Belforte^a, M. Casarsa^a, F. Cossutti^a, G. Della Ricca^{a,b}, C. La Licata^{a,b}, A. Schizzi^{a,b}, A. Zanetti^a

Kyungpook National University, Daegu, Korea

D. H. Kim, G. N. Kim, M. S. Kim, S. Lee, S. W. Lee, Y. D. Oh, S. Sekmen, D. C. Son, Y. C. Yang

Chonbuk National University, Jeonju, Korea

A. Lee

Hanyang University, Seoul, Korea

J. A. Brochero Cifuentes, T. J. Kim

Korea University, Seoul, Korea

S. Cho, S. Choi, Y. Go, D. Gyun, S. Ha, B. Hong, Y. Jo, Y. Kim, B. Lee, K. Lee, K. S. Lee, S. Lee, J. Lim, S. K. Park, Y. Roh

Seoul National University, Seoul, Korea

J. Almond, J. Kim, S. B. Oh, S. h. Seo, U. K. Yang, H. D. Yoo, G. B. Yu

University of Seoul, Seoul, Korea

M. Choi, H. Kim, H. Kim, J. H. Kim, J. S. H. Lee, I. C. Park, G. Ryu, M. S. Ryu

Sungkyunkwan University, Suwon, Korea

Y. Choi, J. Goh, C. Hwang, J. Lee, I. Yu

Vilnius University, Vilnius, Lithuania

V. Dudenė, A. Juodagalvis, J. Vaitkus

National Centre for Particle Physics, Universiti Malaya, Kuala Lumpur, Malaysia

I. Ahmed, Z. A. Ibrahim, J. R. Komaragiri, M. A. B. Md Ali³¹, F. Mohamad Idris³², W. A. T. Wan Abdullah, M. N. Yusli, Z. Zolkapli

Centro de Investigacion y de Estudios Avanzados del IPN, Mexico City, Mexico

H. Castilla-Valdez, E. De La Cruz-Burelo, I. Heredia-De La Cruz³³, A. Hernandez-Almada, R. Lopez-Fernandez, R. Magaña Villalba, J. Mejia Guisao, A. Sanchez-Hernandez

Universidad Iberoamericana, Mexico City, Mexico

S. Carrillo Moreno, C. Oropeza Barrera, F. Vazquez Valencia

Benemerita Universidad Autonoma de Puebla, Puebla, Mexico

S. Carpintero, I. Pedraza, H. A. Salazar Ibarguen, C. Uribe Estrada

Universidad Autónoma de San Luis Potosí, San Luis Potosí, Mexico

A. Morelos Pineda

University of Auckland, Auckland, New Zealand

D. Kofcheck

University of Canterbury, Christchurch, New Zealand

P. H. Butler

National Centre for Physics, Quaid-I-Azam University, Islamabad, Pakistan

A. Ahmad, M. Ahmad, Q. Hassan, H. R. Hoorani, W. A. Khan, M. A. Shah, M. Shoaib, M. Waqas

National Centre for Nuclear Research, Swierk, Poland

H. Bialkowska, M. Bluj, B. Boimska, T. Frueboes, M. Górski, M. Kazana, K. Nawrocki, K. Romanowska-Rybinska, M. Szleper, P. Zalewski

Institute of Experimental Physics, Faculty of Physics, University of Warsaw, Warsaw, Poland

K. Bunkowski, A. Byszuk³⁴, K. Doroba, A. Kalinowski, M. Konecki, J. Krolikowski, M. Misiura, M. Olszewski, M. Walczak

Laboratório de Instrumentação e Física Experimental de Partículas, Lisbon, Portugal

P. Bargassa, C. Beirão Da Cruz E Silva, A. Di Francesco, P. Faccioli, P. G. Ferreira Parracho, M. Gallinaro, J. Hollar, N. Leonardo, L. Lloret Iglesias, M. V. Nemallapudi, J. Rodrigues Antunes, J. Seixas, O. Toldaiev, D. Vadruccio, J. Varela, P. Vischia

Joint Institute for Nuclear Research, Dubna, Russia

P. Bunin, A. Golutvin, I. Golutvin, N. Gorbounov, V. Karjavin, V. Korenkov, A. Lanev, A. Malakhov, V. Matveev^{35,36}, V. V. Mitsyn, P. Moisenz, V. Palichik, V. Perelygin, S. Shmatov, S. Shulha, N. Skatchkov, V. Smirnov, E. Tikhonenko, A. Zarubin

Petersburg Nuclear Physics Institute, Gatchina (St. Petersburg), Russia

L. Chtchipounov, V. Golovtsov, Y. Ivanov, V. Kim³⁷, E. Kuznetsova³⁸, V. Murzin, V. Oreshkin, V. Sulimov, A. Vorobьев

Institute for Nuclear Research, Moscow, Russia

Yu. Andreev, A. Dermenev, S. Glinenko, N. Golubev, A. Karneyeu, M. Kirsanov, N. Krasnikov, A. Pashenkov, D. Tlisov, A. Toropin

Institute for Theoretical and Experimental Physics, Moscow, Russia

V. Epshteyn, V. Gavrilov, N. Lychkovskaya, V. Popov, I. Pozdnyakov, G. Safronov, A. Spiridonov, M. Toms, E. Vlasov, A. Zhokin

Moscow Institute of Physics and Technology, Moscow, Russia

A. Bylinkin³⁶

National Research Nuclear University ‘Moscow Engineering Physics Institute’ (MEPhI), Moscow, RussiaR. Chistov³⁹, M. Danilov³⁹, V. Rusinov**P.N. Lebedev Physical Institute, Moscow, Russia**V. Andreev, M. Azarkin³⁶, I. Dremin³⁶, M. Kirakosyan, A. Leonidov³⁶, S. V. Rusakov, A. Terkulov**Skobeltsyn Institute of Nuclear Physics, Lomonosov Moscow State University, Moscow, Russia**A. Baskakov, A. Belyaev, E. Boos, M. Dubinin⁴⁰, L. Dudko, A. Ershov, A. Gribushin, V. Klyukhin, O. Kodolova, I. Lokhtin, I. Miagkov, S. Obraztsov, S. Petrushanko, V. Savrin, A. Snigirev**Novosibirsk State University (NSU), Novosibirsk, Russia**V. Blinov⁴¹, Y. Skoppen⁴¹**State Research Center of Russian Federation, Institute for High Energy Physics, Protvino, Russia**

I. Azhgirey, I. Bayshev, S. Bitioukov, D. Elumakhov, V. Kachanov, A. Kalinin, D. Konstantinov, V. Krychkine, V. Petrov, R. Ryutin, A. Sobol, S. Troshin, N. Tyurin, A. Uzunian, A. Volkov

Faculty of Physics and Vinca Institute of Nuclear Sciences, University of Belgrade, Belgrade, SerbiaP. Adzic⁴², P. Cirkovic, D. Devetak, M. Dordevic, J. Milosevic, V. Rekovic**Centro de Investigaciones Energéticas Medioambientales y Tecnológicas (CIEMAT), Madrid, Spain**

J. Alcaraz Maestre, M. Barrio Luna, E. Calvo, M. Cerrada, M. Chamizo Llatas, N. Colino, B. De La Cruz, A. Delgado Peris, A. Escalante Del Valle, C. Fernandez Bedoya, J. P. Fernández Ramos, J. Flix, M. C. Fouz, P. Garcia-Abia, O. Gonzalez Lopez, S. Goy Lopez, J. M. Hernandez, M. I. Josa, E. Navarro De Martino, A. Pérez-Calero Yzquierdo, J. Puerta Pelayo, A. Quintario Olmeda, I. Redondo, L. Romero, M. S. Soares

Universidad Autónoma de Madrid, Madrid, Spain

J. F. de Trocóniz, M. Missiroli, D. Moran

Universidad de Oviedo, Oviedo, Spain

J. Cuevas, J. Fernandez Menendez, I. Gonzalez Caballero, J. R. González Fernández, E. Palencia Cortezon, S. Sanchez Cruz, I. Suárez Andrés, J. M. Vizan Garcia

Instituto de Física de Cantabria (IFCA), CSIC-Universidad de Cantabria, Santander, Spain

I. J. Cabrillo, A. Calderon, J. R. Castiñeiras De Saa, E. Curras, M. Fernandez, J. Garcia-Ferrero, G. Gomez, A. Lopez Virto, J. Marco, C. Martinez Rivero, F. Matorras, J. Piedra Gomez, T. Rodrigo, A. Ruiz-Jimeno, L. Scodellaro, N. Trevisani, I. Vila, R. Vilar Cortabitarte

CERN, European Organization for Nuclear Research, Geneva, SwitzerlandD. Abbaneo, E. Auffray, G. Auzinger, M. Bachtis, P. Baillon, A. H. Ball, D. Barney, P. Bloch, A. Bocci, A. Bonato, C. Botta, T. Camporesi, R. Castello, M. Cepeda, G. Cerminara, M. D'Alfonso, D. d'Enterria, A. Dabrowski, V. Daponte, A. David, M. De Gruttola, F. De Guio, A. De Roeck, E. Di Marco⁴³, M. Dobson, B. Dorney, T. du Pree, D. Duggan, M. Dünser, N. Dupont, A. Elliott-Peisert, S. Fartoukh, G. Franzoni, J. Fulcher, W. Funk, D. Gigi, K. Gill, M. Girone, F. Glege, D. Gulhan, S. Gundacker, M. Guthoff, J. Hammer, P. Harris, J. Hegeman, V. Innocente, P. Janot, H. Kirschenmann, V. Knünz, A. Kornmayer¹³, M. J. Kortelainen, K. Kousouris, M. Krammer¹, P. Lecoq, C. Lourenço, M. T. Lucchini, L. Malgeri, M. Mannelli, A. Martelli, F. Meijers, S. Mersi, E. Meschi, F. Moortgat, S. Morovic, M. Mulders, H. Neugebauer, S. Orfanelli, L. Orsini, L. Pape, E. Perez, M. Peruzzi, A. Petrilli, G. Petrucciani, A. Pfeiffer, M. Pierini, A. Racz, T. Reis, G. Rolandi⁴⁴, M. Rovere, M. Ruan, H. Sakulin, J. B. Sauvan, C. Schäfer, C. Schwick, M. Seidel, A. Sharma, P. Silva, M. Simon, P. Sphicas⁴⁵, J. Steggemann, M. Stoye, Y. Takahashi, M. Tosi, D. Treille, A. Triossi, A. Tsirou, V. Veckalns⁴⁶, G. I. Veres²⁰, N. Wardle, H. K. Wöhri, A. Zagozdzinska³⁴, W. D. Zeuner**Paul Scherrer Institut, Villigen, Switzerland**

W. Bertl, K. Deiters, W. Erdmann, R. Horisberger, Q. Ingram, H. C. Kaestli, D. Kotlinski, U. Langenegger, T. Rohe

Institute for Particle Physics, ETH Zurich, Zurich, Switzerland

F. Bachmair, L. Bäni, L. Bianchini, B. Casal, G. Dissertori, M. Dittmar, M. Donegà, P. Eller, C. Grab, C. Heidegger, D. Hits, J. Hoss, G. Kasieczka, P. Lecomte[†], W. Lustermann, B. Mangano, M. Marionneau, P. Martinez Ruiz del Arbol, M. Masciovecchio, M. T. Meinhard, D. Meister, F. Micheli, P. Musella, F. Nessi-Tedaldi, F. Pandolfi, J. Pata, F. Pauss, G. Perrin, L. Perrozzi, M. Quitnat, M. Rossini, M. Schönenberger, A. Starodumov⁴⁷, V. R. Tavolaro, K. Theofilatos, R. Wallny

Universität Zürich, Zurich, Switzerland

T. K. Arrestad, C. Amsler⁴⁸, L. Caminada, M. F. Canelli, A. De Cosa, C. Galloni, A. Hinzmann, T. Hreus, B. Kilminster, C. Lange, J. Ngadiuba, D. Pinna, G. Rauco, P. Robmann, D. Salerno, Y. Yang

National Central University, Chung-Li, Taiwan

V. Candelise, T. H. Doan, Sh. Jain, R. Khurana, M. Konyushikhin, C. M. Kuo, W. Lin, Y. J. Lu, A. Pozdnyakov, S. S. Yu

National Taiwan University (NTU), Taipei, Taiwan

Arun Kumar, P. Chang, Y. H. Chang, Y. W. Chang, Y. Chao, K. F. Chen, P. H. Chen, C. Dietz, F. Fiori, W.-S. Hou, Y. Hsiung, Y. F. Liu, R.-S. Lu, M. Miñano Moya, E. Paganis, A. Psallidas, J. F. Tsai, Y. M. Tzeng

Chulalongkorn University, Faculty of Science, Department of Physics, Bangkok, Thailand

B. Asavapibhop, G. Singh, N. Srimanobhas, N. Suwonjandee

Cukurova University, Adana, Turkey

A. Adiguzel, S. Damarseckin, Z. S. Demiroglu, C. Dozen, E. Eskut, S. Girgis, G. Gokbulut, Y. Guler, E. Gurpinar, I. Hos, E. E. Kangal⁴⁹, O. Kara, U. Kiminsu, M. Oglakci, G. Onengut⁵⁰, K. Ozdemir⁵¹, S. Ozturk⁵², A. Polatoz, D. Sunar Cerci⁵³, B. Tali, S. Turkcapar, I. S. Zorbakir, C. Zorbilmez

Middle East Technical University, Physics Department, Ankara, Turkey

B. Bilin, S. Bilmis, B. Isildak⁵⁴, G. Karapinar⁵⁵, M. Yalvac, M. Zeyrek

Bogazici University, Istanbul, Turkey

E. Gülmez, M. Kaya⁵⁶, O. Kaya⁵⁷, E. A. Yetkin⁵⁸, T. Yetkin⁵⁹

Istanbul Technical University, Istanbul, Turkey

A. Cakir, K. Cankocak, S. Sen⁶⁰

Institute for Scintillation Materials of National Academy of Science of Ukraine, Kharkov, Ukraine

B. Grynyov

National Scientific Center, Kharkov Institute of Physics and Technology, Kharkov, Ukraine

L. Levchuk, P. Sorokin

University of Bristol, Bristol, UK

R. Aggleton, F. Ball, L. Beck, J. J. Brooke, D. Burns, E. Clement, D. Cussans, H. Flacher, J. Goldstein, M. Grimes, G. P. Heath, H. F. Heath, J. Jacob, L. Kreczko, C. Lucas, D. M. Newbold⁶¹, S. Paramesvaran, A. Poll, T. Sakuma, S. Seif El Nasr-storey, D. Smith, V. J. Smith

Rutherford Appleton Laboratory, Didcot, UK

K. W. Bell, A. Belyaev⁶², C. Brew, R. M. Brown, L. Calligaris, D. Cieri, D. J. A. Cockerill, J. A. Coughlan, K. Harder, S. Harper, E. Olaiya, D. Petyt, C. H. Shepherd-Themistocleous, A. Thea, I. R. Tomalin, T. Williams

Imperial College, London, UK

M. Baber, R. Bainbridge, O. Buchmuller, A. Bundock, D. Burton, S. Casasso, M. Citron, D. Colling, L. Corpe, P. Dauncey, G. Davies, A. De Wit, M. Della Negra, R. Di Maria, P. Dunne, A. Elwood, D. Futyan, Y. Haddad, G. Hall, G. Iles, T. James, R. Lane, C. Laner, R. Lucas⁶¹, L. Lyons, A.-M. Magnan, S. Malik, L. Mastrolorenzo, J. Nash, A. Nikitenko⁴⁷, J. Pela, B. Penning, M. Pesaresi, D. M. Raymond, A. Richards, A. Rose, C. Seez, S. Summers, A. Tapper, K. Uchida, M. Vazquez Acosta⁶³, T. Virdee¹³, J. Wright, S. C. Zenz

Brunel University, Uxbridge, UK

J. E. Cole, P. R. Hobson, A. Khan, P. Kyberd, D. Leslie, I. D. Reid, P. Symonds, L. Teodorescu, M. Turner

Baylor University, Waco, USA

A. Borzou, K. Call, J. Dittmann, K. Hatakeyama, H. Liu, N. Pastika

The University of Alabama, Tuscaloosa, USA

O. Charaf, S. I. Cooper, C. Henderson, P. Rumerio

Boston University, Boston, USA

D. Arcaro, A. Avetisyan, T. Bose, D. Gastler, D. Rankin, C. Richardson, J. Rohlf, L. Sulak, D. Zou

Brown University, Providence, USA

G. Benelli, E. Berry, D. Cutts, A. Garabedian, J. Hakala, U. Heintz, J. M. Hogan, O. Jesus, E. Laird, G. Landsberg, Z. Mao, M. Narain, S. Piperov, S. Sagir, E. Spencer, R. Syarif

University of California, Davis, Davis, USA

R. Breedon, G. Breto, D. Burns, M. Calderon De La Barca Sanchez, S. Chauhan, M. Chertok, J. Conway, R. Conway, P. T. Cox, R. Erbacher, C. Flores, G. Funk, M. Gardner, W. Ko, R. Lander, C. Mclean, M. Mulhearn, D. Pellett, J. Pilot, F. Ricci-Tam, S. Shalhout, J. Smith, M. Squires, D. Stolp, M. Tripathi, S. Wilbur, R. Yohay

University of California, Los Angeles, USA

R. Cousins, P. Everaerts, A. Florent, J. Hauser, M. Ignatenko, D. Saltzberg, E. Takasugi, V. Valuev, M. Weber

University of California, Riverside, Riverside, USA

K. Burt, R. Clare, J. Ellison, J. W. Gary, G. Hanson, J. Heilman, P. Jandir, E. Kennedy, F. Lacroix, O. R. Long, M. Malberti, M. Olmedo Negrete, M. I. Paneva, A. Shrinivas, H. Wei, S. Wimpenny, B. R. Yates

University of California, San Diego, La Jolla, USA

J. G. Branson, G. B. Cerati, S. Cittolin, M. Derdzinski, R. Gerosa, A. Holzner, D. Klein, V. Krutelyov, J. Letts, I. Macneill, D. Olivito, S. Padhi, M. Pieri, M. Sani, V. Sharma, S. Simon, M. Tadel, A. Vartak, S. Wasserbaech⁶⁴, C. Welke, J. Wood, F. Würthwein, A. Yagil, G. Zevi Della Porta

Department of Physics, University of California, Santa Barbara, Santa Barbara, USA

R. Bhandari, J. Bradmiller-Feld, C. Campagnari, A. Dishaw, V. Dutta, K. Flowers, M. Franco Sevilla, P. Geffert, C. George, F. Golf, L. Gouskos, J. Gran, R. Heller, J. Incandela, N. Mccoll, S. D. Mullin, A. Ovcharova, J. Richman, D. Stuart, I. Suarez, C. West, J. Yoo

California Institute of Technology, Pasadena, USA

D. Anderson, A. Apresyan, J. Bendavid, A. Bornheim, J. Bunn, Y. Chen, J. M. Lawhorn, A. Mott, H. B. Newman, C. Pena, M. Spiropulu, J. R. Vlimant, S. Xie, R. Y. Zhu

Carnegie Mellon University, Pittsburgh, USA

M. B. Andrews, V. Azzolini, B. Carlson, T. Ferguson, M. Paulini, J. Russ, M. Sun, H. Vogel, I. Vorobiev

University of Colorado Boulder, Boulder, USA

J. P. Cumalat, W. T. Ford, F. Jensen, A. Johnson, M. Krohn, T. Mulholland, K. Stenson, S. R. Wagner

Cornell University, Ithaca, USA

J. Alexander, J. Chaves, J. Chu, S. Dittmer, K. Mcdermott, N. Mirman, G. Nicolas Kaufman, J. R. Patterson, A. Rinkevicius, A. Ryd, L. Skinnari, L. Soffi, S. M. Tan, Z. Tao, J. Thom, J. Tucker, P. Wittich, M. Zientek

Fairfield University, Fairfield, USA

D. Winn

Fermi National Accelerator Laboratory, Batavia, USA

S. Abdullin, M. Albrow, G. Apollinari, S. Banerjee, L. A. T. Bauerick, A. Beretvas, J. Berryhill, P. C. Bhat, G. Bolla, K. Burkett, J. N. Butler, H. W. K. Cheung, F. Chlebana, S. Cihangir[†], M. Cremonesi, V. D. Elvira, I. Fisk, J. Freeman, E. Gottschalk, L. Gray, D. Green, S. Grünendahl, O. Gutsche, D. Hare, R. M. Harris, S. Hasegawa, J. Hirschauer, Z. Hu, B. Jayatilaka, S. Jindariani, M. Johnson, U. Joshi, B. Klima, B. Kreis, S. Lammel, J. Linacre, D. Lincoln, R. Lipton, T. Liu, R. Lopes De Sá, J. Lykken, K. Maeshima, N. Magini, J. M. Marraffino, S. Maruyama, D. Mason, P. McBride, P. Merkel, S. Mrenna, S. Nahn, C. Newman-Holmes[†], V. O'Dell, K. Pedro, O. Prokofyev, G. Rakness, L. Ristori, E. Sexton-Kennedy, A. Soha, W. J. Spalding, L. Spiegel, S. Stoynev, N. Strobbe, L. Taylor, S. Tkaczyk, N. V. Tran, L. Uplegger, E. W. Vaandering, C. Vernieri, M. Verzocchi, R. Vidal, M. Wang, H. A. Weber, A. Whitbeck

University of Florida, Gainesville, USA

D. Acosta, P. Avery, P. Bortignon, D. Bourilkov, A. Brinkerhoff, A. Carnes, M. Carver, D. Curry, S. Das, R. D. Field, I. K. Furic, J. Konigsberg, A. Korytov, P. Ma, K. Matchev, H. Mei, P. Milenovic⁶⁵, G. Mitselmakher, D. Rank, L. Shchutska, D. Sperka, L. Thomas, J. Wang, S. Wang, J. Yelton

Florida International University, Miami, USA

S. Linn, P. Markowitz, G. Martinez, J. L. Rodriguez

Florida State University, Tallahassee, USA

A. Ackert, J. R. Adams, T. Adams, A. Askew, S. Bein, B. Diamond, S. Hagopian, V. Hagopian, K. F. Johnson, A. Khatiwada, H. Prosper, A. Santra, M. Weinberg

Florida Institute of Technology, Melbourne, USA

M. M. Baarmand, V. Bhopatkar, S. Colafranceschi⁶⁶, M. Hohlmann, D. Noonan, T. Roy, F. Yumiceva

University of Illinois at Chicago (UIC), Chicago, USA

M. R. Adams, L. Apanasevich, D. Berry, R. R. Betts, I. Bucinskaite, R. Cavanaugh, O. Evdokimov, L. Gauthier, C. E. Gerber, D. J. Hofman, P. Kurt, C. O'Brien, I. D. Sandoval Gonzalez, P. Turner, N. Varelas, H. Wang, Z. Wu, M. Zakaria, J. Zhang

The University of Iowa, Iowa City, USA

B. Bilki⁶⁷, W. Clarida, K. Dilsiz, S. Durgut, R. P. Gandrajula, M. Haytmyradov, V. Khristenko, J.-P. Merlo, H. Mermerkaya⁶⁸, A. Mestvirishvili, A. Moeller, J. Nachtman, H. Ogul, Y. Onel, F. Ozok⁶⁹, A. Penzo, C. Snyder, E. Tiras, J. Wetzel, K. Yi

Johns Hopkins University, Baltimore, USA

I. Anderson, B. Blumenfeld, A. Cocoros, N. Eminizer, D. Fehling, L. Feng, A. V. Gritsan, P. Maksimovic, M. Osherson, J. Roskes, U. Sarica, M. Swartz, M. Xiao, Y. Xin, C. You

The University of Kansas, Lawrence, USA

A. Al-bataineh, P. Baringer, A. Bean, J. Bowen, C. Bruner, J. Castle, R. P. Kenny III, A. Kropivnitskaya, D. Majumder, W. Mcbrayer, M. Murray, S. Sanders, R. Stringer, J. D. Tapia Takaki, Q. Wang

Kansas State University, Manhattan, USA

A. Ivanov, K. Kaadze, S. Khalil, M. Makouski, Y. Maravin, A. Mohammadi, L. K. Saini, N. Skhirtladze, S. Toda

Lawrence Livermore National Laboratory, Livermore, USA

D. Lange, F. Rebassoo, D. Wright

University of Maryland, College Park, USA

C. Anelli, A. Baden, O. Baron, A. Belloni, B. Calvert, S. C. Eno, C. Ferraioli, J. A. Gomez, N. J. Hadley, S. Jabeen, R. G. Kellogg, T. Kolberg, J. Kunkle, Y. Lu, A. C. Mignerey, Y. H. Shin, A. Skuja, M. B. Tonjes, S. C. Tonwar

Massachusetts Institute of Technology, Cambridge, USA

D. Abercrombie, B. Allen, A. Apyan, R. Barbieri, A. Baty, R. Bi, K. Bierwagen, S. Brandt, W. Busza, I. A. Cali, Z. Demiragli, L. Di Matteo, G. Gomez Ceballos, M. Goncharov, D. Hsu, Y. Iiyama, G. M. Innocenti, M. Klute, D. Kovalskyi, K. Krajezar, Y. S. Lai, Y.-J. Lee, A. Levin, P. D. Luckey, A. C. Marini, C. McGinn, C. Mironov, S. Narayanan, X. Niu, C. Paus, C. Roland, G. Roland, J. Salfeld-Nebgen, G. S. F. Stephans, K. Sumorok, K. Tatar, M. Varma, D. Velicanu, J. Veverka, J. Wang, T. W. Wang, B. Wyslouch, M. Yang, V. Zhukova

University of Minnesota, Minneapolis, USA

A. C. Benvenuti, R. M. Chatterjee, A. Evans, A. Finkel, A. Gude, P. Hansen, S. Kalafut, S. C. Kao, Y. Kubota, Z. Lesko, J. Mans, S. Nourbakhsh, N. Ruckstuhl, R. Rusack, N. Tambe, J. Turkewitz

University of Mississippi, Oxford, USA

J. G. Acosta, S. Oliveros

University of Nebraska-Lincoln, Lincoln, USA

E. Avdeeva, R. Bartek, K. Bloom, S. Bose, D. R. Claes, A. Dominguez, C. Fangmeier, R. Gonzalez Suarez, R. Kamalieddin, D. Knowlton, I. Kravchenko, A. Malta Rodrigues, F. Meier, J. Monroy, J. E. Siado, G. R. Snow, B. Stieger

State University of New York at Buffalo, Buffalo, USA

M. Alyari, J. Dolen, J. George, A. Godshalk, C. Harrington, I. Iashvili, J. Kaisen, A. Kharchilava, A. Kumar, A. Parker, S. Rappoccio, B. Roozbahani

Northeastern University, Boston, USA

G. Alverson, E. Barberis, D. Baumgartel, A. Hortiangtham, B. Knapp, A. Massironi, D. M. Morse, D. Nash, T. Orimoto, R. Teixeira De Lima, D. Trocino, R.-J. Wang, D. Wood

Northwestern University, Evanston, USA

S. Bhattacharya, K. A. Hahn, A. Kubik, A. Kumar, J. F. Low, N. Mucia, N. Odell, B. Pollack, M. H. Schmitt, K. Sung, M. Trovato, M. Velasco

University of Notre Dame, Notre Dame, USA

N. Dev, M. Hildreth, K. Hurtado Anampa, C. Jessop, D. J. Karmgard, N. Kellams, K. Lannon, N. Marinelli, F. Meng, C. Mueller, Y. Musienko³⁵, M. Planer, A. Reinsvold, R. Ruchti, G. Smith, S. Taroni, N. Valls, M. Wayne, M. Wolf, A. Woodard

The Ohio State University, Columbus, USA

J. Alimena, L. Antonelli, J. Brinson, B. Bylsma, L. S. Durkin, S. Flowers, B. Francis, A. Hart, C. Hill, R. Hughes, W. Ji, B. Liu, W. Luo, D. Puigh, B. L. Winer, H. W. Wulsin

Princeton University, Princeton, USA

S. Cooperstein, O. Driga, P. Elmer, J. Hardenbrook, P. Hebda, J. Luo, D. Marlow, T. Medvedeva, K. Mei, M. Mooney, J. Olsen, C. Palmer, P. Piroué, D. Stickland, C. Tully, A. Zuranski

University of Puerto Rico, Mayaguez, USA

S. Malik

Purdue University, West Lafayette, USA

A. Barker, V. E. Barnes, S. Folgueras, L. Gutay, M. K. Jha, M. Jones, A. W. Jung, K. Jung, D. H. Miller, N. Neumeister, B. C. Radburn-Smith, X. Shi, J. Sun, A. Svyatkovskiy, F. Wang, W. Xie, L. Xu

Purdue University Calumet, Hammond, USA

N. Parashar, J. Stupak

Rice University, Houston, USA

A. Adair, B. Akgun, Z. Chen, K. M. Ecklund, F. J. M. Geurts, M. Guilbaud, W. Li, B. Michlin, M. Northup, B. P. Padley, R. Redjimi, J. Roberts, J. Rorie, Z. Tu, J. Zabel

University of Rochester, Rochester, USA

B. Betchart, A. Bodek, P. de Barbaro, R. Demina, Y. t. Duh, T. Ferbel, M. Galanti, A. Garcia-Bellido, J. Han, O. Hindrichs, A. Khukhunaishvili, K. H. Lo, P. Tan, M. Verzetti

Rutgers, The State University of New Jersey, Piscataway, USA

J. P. Chou, E. Contreras-Campana, Y. Gershtein, T. A. Gómez Espinosa, E. Halkiadakis, M. Heindl, D. Hidas, E. Hughes, S. Kaplan, R. Kunnnawalkam Elayavalli, S. Kyriacou, A. Lath, K. Nash, H. Saka, S. Salur, S. Schnetzer, D. Sheffield, S. Somalwar, R. Stone, S. Thomas, P. Thomassen, M. Walker

University of Tennessee, Knoxville, USA

M. Foerster, J. Heideman, G. Riley, K. Rose, S. Spanier, K. Thapa

Texas A&M University, College Station, USA

O. Bouhali⁷⁰, A. Celik, M. Dalchenko, M. De Mattia, A. Delgado, S. Dildick, R. Eusebi, J. Gilmore, T. Huang, E. Juska, T. Kamon⁷¹, R. Mueller, Y. Pakhotin, R. Patel, A. Perloff, L. Perniè, D. Rathjens, A. Rose, A. Safonov, A. Tatarinov, K. A. Ulmer

Texas Tech University, Lubbock, USA

N. Akchurin, C. Cowden, J. Damgov, C. Dragoiu, P. R. Dudero, J. Faulkner, S. Kunori, K. Lamichhane, S. W. Lee, T. Libeiro, S. Undleeb, I. Volobouev, Z. Wang

Vanderbilt University, Nashville, USA

A. G. Delannoy, S. Greene, A. Gurrola, R. Janjam, W. Johns, C. Maguire, A. Melo, H. Ni, P. Sheldon, S. Tuo, J. Velkovska, Q. Xu

University of Virginia, Charlottesville, USA

M. W. Arenton, P. Barria, B. Cox, J. Goodell, R. Hirosky, A. Ledovskoy, H. Li, C. Neu, T. Sinthuprasith, X. Sun, Y. Wang, E. Wolfe, F. Xia

Wayne State University, Detroit, USA

C. Clarke, R. Harr, P. E. Karchin, P. Lamichhane, J. Sturdy

University of Wisconsin-Madison, Madison, WI, USA

D. A. Belknap, S. Dasu, L. Dodd, S. Duric, B. Gomber, M. Grothe, M. Herndon, A. Hervé, P. Klabbers, A. Lanaro, A. Levine, K. Long, R. Loveless, I. Ojalvo, T. Perry, G. A. Pierro, G. Polese, T. Ruggles, A. Savin, A. Sharma, N. Smith, W. H. Smith, D. Taylor, N. Woods

† Deceased

- 1: Also at Vienna University of Technology, Vienna, Austria
- 2: Also at State Key Laboratory of Nuclear Physics and Technology, Peking University, Beijing, China
- 3: Also at Institut Pluridisciplinaire Hubert Curien, Université de Strasbourg, Université de Haute Alsace Mulhouse, CNRS/IN2P3, Strasbourg, France
- 4: Also at Universidade Estadual de Campinas, Campinas, Brazil
- 5: Also at Universidade Federal de Pelotas, Pelotas, Brazil
- 6: Also at Université Libre de Bruxelles, Brussels, Belgium
- 7: Also at Deutsches Elektronen-Synchrotron, Hamburg, Germany
- 8: Also at Joint Institute for Nuclear Research, Dubna, Russia
- 9: Now at British University in Egypt, Cairo, Egypt
- 10: Also at Zewail City of Science and Technology, Zewail, Egypt
- 11: Now at Ain Shams University, Cairo, Egypt
- 12: Also at Université de Haute Alsace, Mulhouse, France
- 13: Also at CERN, European Organization for Nuclear Research, Geneva, Switzerland
- 14: Also at Skobeltsyn Institute of Nuclear Physics, Lomonosov Moscow State University, Moscow, Russia
- 15: Also at Tbilisi State University, Tbilisi, Georgia
- 16: Also at RWTH Aachen University, III. Physikalisches Institut A, Aachen, Germany
- 17: Also at University of Hamburg, Hamburg, Germany
- 18: Also at Brandenburg University of Technology, Cottbus, Germany
- 19: Also at Institute of Nuclear Research ATOMKI, Debrecen, Hungary
- 20: Also at MTA-ELTE Lendület CMS Particle and Nuclear Physics Group, Eötvös Loránd University, Budapest, Hungary
- 21: Also at University of Debrecen, Debrecen, Hungary

- 22: Also at Indian Institute of Science Education and Research, Bhopal, India
23: Also at Institute of Physics, Bhubaneswar, India
24: Also at University of Visva-Bharati, Santiniketan, India
25: Also at University of Ruhuna, Matara, Sri Lanka
26: Also at Isfahan University of Technology, Isfahan, Iran
27: Also at University of Tehran, Department of Engineering Science, Tehran, Iran
28: Also at Plasma Physics Research Center, Science and Research Branch, Islamic Azad University, Tehran, Iran
29: Also at Università degli Studi di Siena, Siena, Italy
30: Also at Purdue University, West Lafayette, USA
31: Also at International Islamic University of Malaysia, Kuala Lumpur, Malaysia
32: Also at Malaysian Nuclear Agency, MOSTI, Kajang, Malaysia
33: Also at Consejo Nacional de Ciencia y Tecnología, Mexico city, Mexico
34: Also at Warsaw University of Technology, Institute of Electronic Systems, Warsaw, Poland
35: Also at Institute for Nuclear Research, Moscow, Russia
36: Now at National Research Nuclear University ‘Moscow Engineering Physics Institute’ (MEPhI), Moscow, Russia
37: Also at St. Petersburg State Polytechnical University, St. Petersburg, Russia
38: Also at University of Florida, Gainesville, USA
39: Also at P.N. Lebedev Physical Institute, Moscow, Russia
40: Also at California Institute of Technology, Pasadena, USA
41: Also at Budker Institute of Nuclear Physics, Novosibirsk, Russia
42: Also at Faculty of Physics, University of Belgrade, Belgrade, Serbia
43: Also at INFN Sezione di Roma; Università di Roma, Rome, Italy
44: Also at Scuola Normale e Sezione dell'INFN, Pisa, Italy
45: Also at National and Kapodistrian University of Athens, Athens, Greece
46: Also at Riga Technical University, Riga, Latvia
47: Also at Institute for Theoretical and Experimental Physics, Moscow, Russia
48: Also at Albert Einstein Center for Fundamental Physics, Bern, Switzerland
49: Also at Mersin University, Mersin, Turkey
50: Also at Cag University, Mersin, Turkey
51: Also at Piri Reis University, Istanbul, Turkey
52: Also at Gaziosmanpasa University, Tokat, Turkey
53: Also at Adiyaman University, Adiyaman, Turkey
54: Also at Ozyegin University, Istanbul, Turkey
55: Also at Izmir Institute of Technology, Izmir, Turkey
56: Also at Marmara University, Istanbul, Turkey
57: Also at Kafkas University, Kars, Turkey
58: Also at Istanbul Bilgi University, Istanbul, Turkey
59: Also at Yildiz Technical University, Istanbul, Turkey
60: Also at Hacettepe University, Ankara, Turkey
61: Also at Rutherford Appleton Laboratory, Didcot, UK
62: Also at School of Physics and Astronomy, University of Southampton, Southampton, UK
63: Also at Instituto de Astrofísica de Canarias, La Laguna, Spain
64: Also at Utah Valley University, Orem, USA
65: Also at University of Belgrade, Faculty of Physics and Vinca Institute of Nuclear Sciences, Belgrade, Serbia
66: Also at Facoltà Ingegneria, Università di Roma, Rome, Italy
67: Also at Argonne National Laboratory, Argonne, USA
68: Also at Erzincan University, Erzincan, Turkey
69: Also at Mimar Sinan University, Istanbul, Istanbul, Turkey
70: Also at Texas A&M University at Qatar, Doha, Qatar
71: Also at Kyungpook National University, Daegu, Korea